

---

Theses and Dissertations

---

2010

# Experimental investigation of initiation of cool flame in flow reactor

Jun-Chun Wong  
*University of Iowa*

Copyright 2010 Jun-Chun Wong

This thesis is available at Iowa Research Online: <http://ir.uiowa.edu/etd/1279>

---

## Recommended Citation

Wong, Jun-Chun. "Experimental investigation of initiation of cool flame in flow reactor." MS (Master of Science) thesis, University of Iowa, 2010.  
<http://ir.uiowa.edu/etd/1279>.

---

Follow this and additional works at: <http://ir.uiowa.edu/etd>

 Part of the [Mechanical Engineering Commons](#)

EXPERIMENTAL INVESTIGATION OF INITIATION OF COOL FLAME IN FLOW  
REACTOR

by  
Jun-Chun Wong

A thesis submitted in partial fulfillment  
of the requirements for the Master of  
Science degree in Mechanical Engineering  
in the Graduate College of  
The University of Iowa

July 2010

Thesis Supervisor: Professor Lea-Der Chen

Graduate College  
The University of Iowa  
Iowa City, Iowa

CERTIFICATE OF APPROVAL

---

MASTER'S THESIS

---

This is to certify that the Master's thesis of

Jun-Chun Wong

has been approved by the Examining Committee  
for the thesis requirement for the Master of  
Science degree in Mechanical Engineering at  
the July 2010 graduation.

Thesis Committee: \_\_\_\_\_  
Lea-Der Chen, Thesis Supervisor

\_\_\_\_\_  
Albert Ratner

\_\_\_\_\_  
Ching-Long Lin

## ACKNOWLEDGMENTS

The author wishes to thank Professor L.D. Chen for all his patience and guidance advising this thesis project. With his support, the project went forward smoothly. The author also learned skills of performing experiments and methods of conducting research. I would also like to thank my lab partners (Ankush Bhasin, Ryan Cappaert, Dan Wu and Scott Ruebush) who always helped me when some difficulties came up. Lastly, thanks to his parents, Mr. & Mrs. Wong, to support him to study in the University of Iowa and the writing of this thesis.

This research was supported, in part, by ConocoPhillips. The author also wishes to acknowledge insightful discussion with Dr. Garry Gunter and Dr. Sergei Filatyev at ConocoPhillips Technical Center, Bartlesville, Oklahoma.

## ABSTRACT

A horizontal flow reactor to conduct cool flame experiment has been set up and the experiment has been conducted. Different reactor materials and testing conditions have been tried to create the best environment for hydrocarbon (PRF0, PRF65 and PRF85) cool flame oxidation. Temperature oscillation range and position has been recorded by 21 thermocouples. Three trials have been performed to discover the correlation between temperature change and cool flame position. Finally, the suitable conditions for cool flame oxidation have been obtained. Relation between octane number and cool flame characteristic has also been discussed.

## TABLE OF CONTENTS

LIST OF TABLES .....	v
LIST OF FIGURES .....	vi
CHAPTER	
1. INTRODUCTION.....	1
1.1. Octane Number.....	1
1.2. Cool Flame.....	2
1.3. Octane Number Determination.....	4
2. EXPERIMENTAL METHOD.....	5
2.1. Experimental Setup.....	5
2.1.1 Fuel/Air Feed System .....	6
2.1.2 Fuel/Air Vaporizer.....	7
2.1.3 Flow Reactor .....	8
2.1.4 Exhaust Burn-off .....	10
2.1.5 Mass Flow Meter Recalibration .....	12
2.2. Experimental Procedure.....	13
2.3. Data Acquisition and Arrangement .....	14
3. RESULT AND DISCUSSION .....	19
3.1. Illumination and Temperature Rise in Different Material Reactors.....	19
3.2. Suitable Conditions for the Experiment .....	23
3.3. Comparisons and Discussions of the 3 Trials.....	31
4. CONCLUSIONS AND RECOMMENDATIONS .....	37
4.1. Summary of Conclusions.....	37
4.2. Future Works and Recommendations.....	37
REFERENCES.....	39

## LIST OF TABLES

Table 2-1: Thermocouple Positions in the Reactor.....	9
Table 2-2: Description of the Exhaust Burn-off Section .....	11
Table 2-3: Fuel Composition .....	13
Table 3-1: Fixing ER=1.06, Changing Mixture Velocity (PRF0, PRF100).....	20
Table 3-2: Fixing ER=1.06, Changing Mixture Velocity (PRF0, PRF100).....	20
Table 3-3: Fixing Mixture Velocity at 0.0197m/s, Changing Equivalence Ration (PRF0 and PRF100).....	20
Table 3-4: Testing Condition of the Successful Trial.....	22
Table 3-5: Testing Condition of the Most Clear Temperature Oscillation.....	28

## LIST OF FIGURES

Figure 1-1: Cool flame and two-stage ignition limit of C <sub>3</sub> H <sub>8</sub> + O <sub>2</sub> in a silica vessel of 5.5 cm diameter. Propane : oxygen ratio, 1:1 .....	3
Figure 2-1: Experimental Setup Diagram .....	5
Figure 2-2: Experimental Setup .....	6
Figure 2-3: Syringe between the Pump and Fuel Tank.....	7
Figure 2-4: Flow Conditioning and Flame Arrester Section .....	9
Figure 2-5: Drilled Reactor Tube.....	10
Figure 2-6: The Exhaust Burn-off Section.....	11
Figure 2-7: Fuel Burn Off at the Reactor Exit .....	11
Figure 2-8: AFM2600 Mass Flow Meter Calibration.....	12
Figure 2-9: Interface of DasyLab.....	15
Figure 2-10: Temperature Data Saved in Excel File .....	16
Figure 2-11: Reactor Thermocouples at Room Temperature .....	17
Figure 2-12: Reactor Thermocouples when Furnace Was Set to 345C.....	17
Figure 2-13: Temperature Oscillation at Each Thermocouple Taking One Minute time interval .....	18
Figure 3-1: Temperature Oscillation at Middle of Reactor and Outlet.....	21
Figure 3-2: Yellow Deposits on Reactor Wall.....	22
Figure 3-3: Temperature Oscillation of Thermocouple 1-10 (v= 0.1 m/s, Inlet Temperature 182C, Furnace Temperature 350C.).....	24
Figure 3-4: Temperature Oscillation of Thermocouple 11-21 (v= 0.1 m/s, Inlet Temperature 182C, Furnace Temperature 350C.).....	24
Figure 3-5: Temperature Oscillation in the Reactor Per Minute (v= 0.1 m/s, Inlet Temperature 182C, Furnace Temperature 350C.).....	25
Figure 3-6: Temperature Oscillation of Thermocouple 1-10 (v= 0.085 m/s, Inlet Temperature 182C, Furnace Temperature 350C.).....	25
Figure 3-7: Temperature Oscillation of Thermocouple 11-21 (v= 0.085 m/s, Inlet Temperature 182C, Furnace Temperature 350C.).....	26



Figure 3-8: Temperature Oscillation of Thermocouple 1-10 ( $v= 0.085$ m/s, Inlet Temperature 182C, Furnace Temperature 345C.).....	26
Figure 3-9: Temperature Oscillation of Thermocouple 11-21 ( $v= 0.085$ m/s, Inlet Temperature 182C, Furnace Temperature 345C.).....	27
Figure 3-10: Temperature Oscillation in the Reactor Every 15 Seconds ( $v= 0.085$ m/s, Inlet Temperature 182C, Furnace Temperature 345C.).....	27
Figure 3-11: Temperature Oscillation of Thermocouple 1-10 ( $v= 0.05$ m/s, Inlet Temperature 182C, Furnace Temperature 345C.).....	29
Figure 3-12: Temperature Oscillation of Thermocouple 11-21 ( $v= 0.05$ m/s, Inlet Temperature 182C, Furnace Temperature 345C.).....	29
Figure 3-13: Temperature Oscillation in the Reactor ( $v= 0.05$ m/s, Inlet Temperature 182C, Furnace Temperature 345C.).....	30
Figure 3-14: Temperature Oscillation at the 8th Thermocouple ( $v= 0.05$ m/s, Inlet Temperature 182C, Furnace Temperature 345C.).....	30
Figure 3-15: The Initial Cool Flame Positions and Temperature Rise of Trial #1 .....	32
Figure 3-16: The Maximum Temperature Change Positions and Range of Trial #1 .....	32
Figure 3-17: The Initial Cool Flame Positions and Temperature Rise of Trial #2 .....	33
Figure 3-18: The Maximum Temperature Change Positions and Range of Trial #2 .....	33
Figure 3-19: The Initial Cool Flame Positions and Temperature Rise of Trial #3 .....	34
Figure 3-20: The Maximum Temperature Change Positions and Range of Trial #3 .....	34
Figure 3-21: Initial Cool flame Temperature Rising Range for 3 Trials .....	36
Figure 3-22: Maximum Temperature Rising Range for 3 Trials .....	36

## CHAPTER 1: INTRODUCTION

### **1.1 Octane Number**

Octane number is used to rank the antiknock property of automotive fuels for spark ignition or gasoline engines. Ideally, when the spark ignites the fuel-air mixture in the cylinder, the flame front spreads out smoothly from the spark into the unburned fuel-air mixture, giving a gradual increase of pressure that pushes to the piston work is delivered. However, engine knock can occur when the engine compression ratio exceeds the antiknock limit of the fuel-air mixture that is self-ignition takes place before the spark is actuated. As self-ignited flame front spreads, hot combustion products behind the flame front compress the unburned fuel-air mixture, resulting in an increase of temperature. Radiation and conduction from the burnt mixture also increase the temperature of the unburned fuel-air mixture. When the unburnt mixture reaches its ignition temperature, spontaneous ignition occurs and results on uncontrolled ignition and combustion known as the engine knock phenomena, resulting in decrease of thermal efficiency and damages to engines (Amann et al., 1989).

Octane number is used to quantify the fuel antiknock property. The higher the octane number is, the fuel can be used in higher compression ratio engines. However, proper octane number fuels should be used per specifications of the engines to avoid engine damages or performance degradation (Nader, 1970). Using lower octane number fuels than specified will result in bearing wear, piston cracking and valve damages due to engine knock. The hydrocarbon smog output will also increase because of incomplete combustion of the fuel. On the other hand, when the fuel with a higher than specified octane number is used, the pollution will increase if lead compounds or aromatics are blended in the fuel mixture not to mention the premier paid for higher octane number fuels.

Standard test procedure was developed for determining octane number in the 1960s (Drews et al., 1998). Isooctane (2, 2, 4-trimethylpentane) was chosen as a reference fuel with an assigned octane number of 100. The straight chain n-heptane was given an octane number of zero due to its poor anti-knocking property. The octane number of a fuel is described as the percent by volume of isooctane that must be blended with n-heptane to produce a blend having the same anti-knocking characteristics as the gasoline under study (Ingersoll, 1995). The octane number of a gasoline is determined by comparing its performance engine tests with the performance of a mixture of isooctane and n-heptane. The proportions of the mixture are varied until the mixture produces a knock of same intensity as that produced by gasoline.

Two octane rating methods are commonly used: MON (Motor Octane Number) and RON (Research Octane Number) (McKetta, 1976). Same reference fuel and same engine are used, but the test conditions are different. For RON testing, a fixed spark advance angle is set, and it has a lower inlet temperature and a lower engine speed than MON testing. For MON testing, a variable spark timing and higher mixture temperature and faster engine speed are used. The averaged values of RON and MON testing, also known as Anti Knocking Index (AKI), were commonly used to characterize the anti-knocking properties of the fuels.

## **1.2 Cool Flame**

Ignition of hydrocarbon-air mixtures can exhibit two-stage phenomena (Mantashyan et al., 1979). Namely, a low temperature oxidation and followed by a high temperature, exothermic process, e.g., see Figure 1-1. The low temperature oxidation, also known as cool flame, is primarily due to the chain branching reactions in the mixture. It is important to gain good understanding of the cool flame as it is related to the engine knock phenomena.

There are many parameters that can have an impact on the presence of cool flames, For example, the fuel structure, system temperature and pressure, the reaction chamber surface properties, and methods of ignition can impact the presence or not of the cool flame (Turns, 2000).

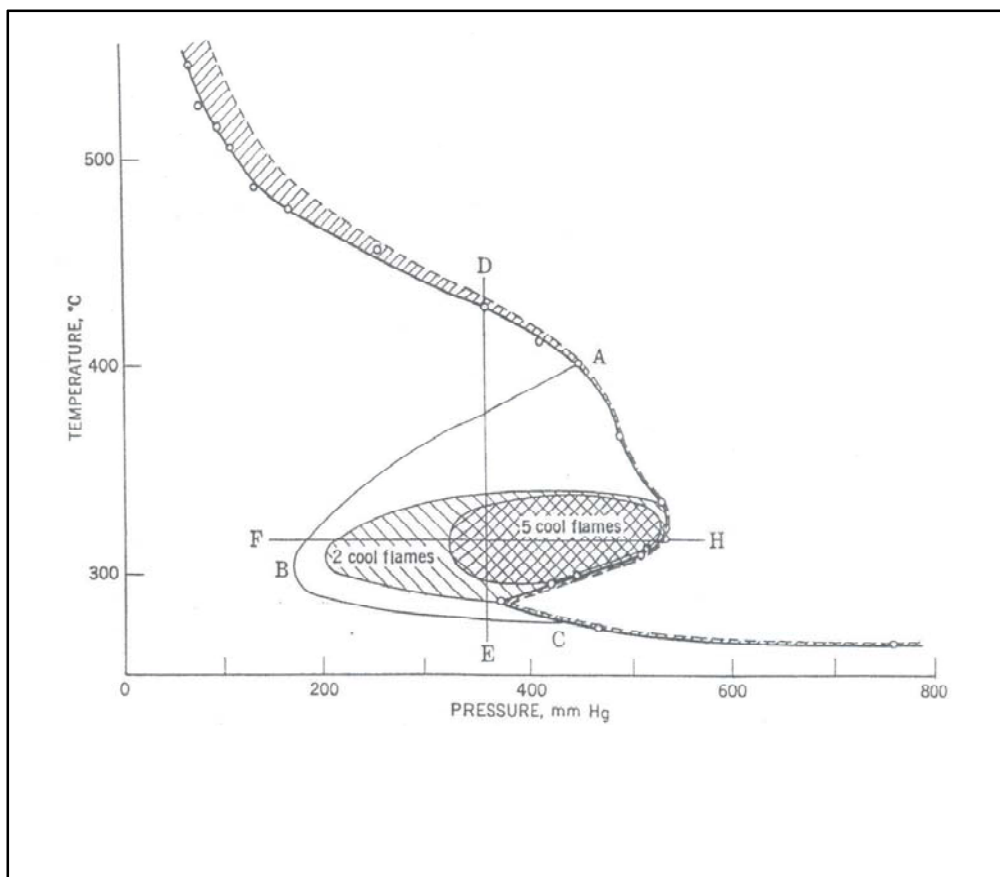


Figure 1-1: Cool flame and two-stage ignition limit of  $C_3H_8 + O_2$  in a silica vessel of 5.5 cm diameter. Propane : oxygen ratio, 1:1

Source: Elbe, Guenther von, and Bernard Lewis. *Combustion, Flames and Explosions of Gases, Third Edition*. 3 ed. Toronto: Academic Press, 1987.

### **1.3 Octane Number Determination**

In addition to engine-based test methods summarized in the Section 1.1, other methods were developed to correlate octane number with physical or chemical properties

of the mixture such as the electrophysical methods used by Pushkin et al. (2002) and near infrared spectral data examined by Kelly et al. (1989).

Experiments were also conducted in rapid compression machines or in a flat-flame environment to correlate the induction time or ignition delay with octane number (Griffiths et al., 1984), as well as in isothermal, cylindrical reactors (Stepanskii et al., 1981 and Fenske et al., 1969). We adopted the cylindrical reactor in current study, partly because of the simplicity in the experiments and partly because of major equipment being readily available in the lab. The isothermal reactor can be modified to examine the catalytic effects in initiation of cool flames for future studies.

## CHAPTER 2: EXPERIMENTAL METHOD

### 2.1 Experimental Setup

The experimental set-up consists of 4 major sections: (a) fuel/air feed system, (b) fuel vaporizer, (c) flow reactor, and (d) exhaust burn-off, as shown in Figures 2-1 and 2-2.

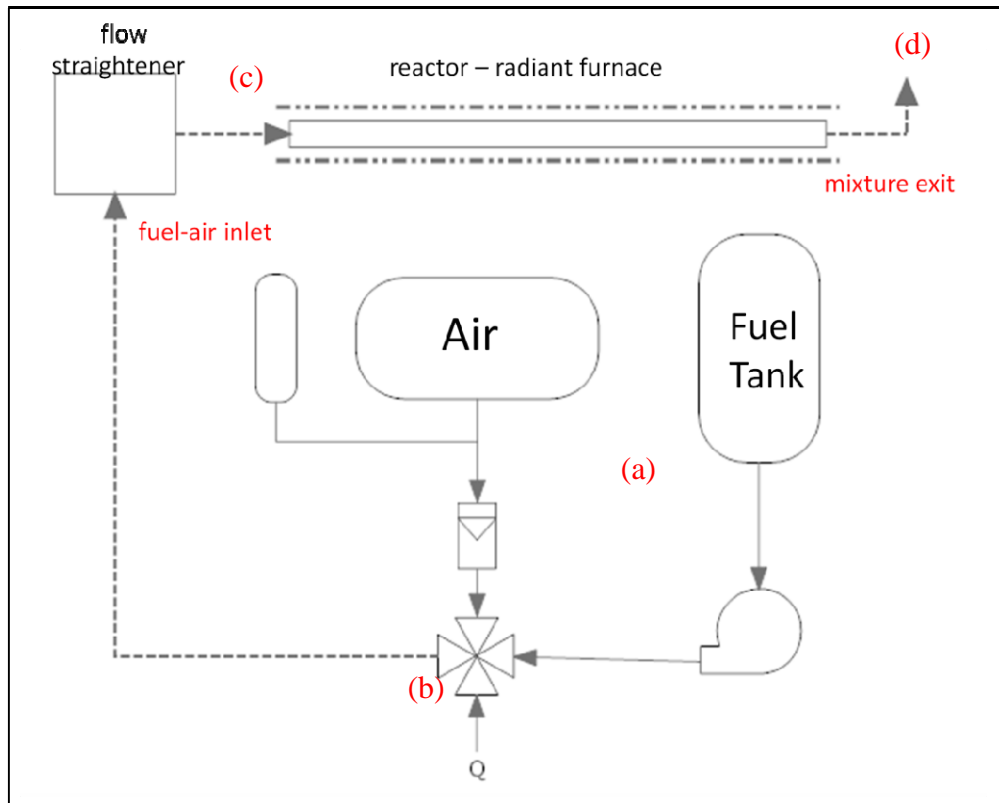


Figure 2-1: Experimental Setup Diagram

Fuel and air were fed in section (a), premixed and vaporized in section (b), and then entered section (c) for conditioning and principal experimental testing. The unburned fuel was burned off at the exhaust, section (d).



Figure 2-2: Experimental Setup

### 2.1.1 Fuel/Air Feed System

A Gilson 305 pump with 5-SC piston head was used to deliver liquid fuels. The fuel flow rate ranged from 0.01 to 5 ml/min. Building air was used and the flowrate was monitored by a mass flow meter, AALBORG AFM2600 in conjunction with an AALBORG PROM mass flow meter indicator, showing the percentage of maximum flow of AFM2600 (15 l/min). An air canister was parallel connected to the air feeding line as a capacitive controller in order to make the air flow more stable.

Sometimes when the pump started pumping, bubbles produced gaps in between of the pump and fuel tank. Thus, a syringe is connected between them to reduce bubble. While bubbles appeared in the fuel line, turn the syringe valve to “Syringe Load position”,

as shown in Figure 2-3, and draw the bubbles and liquid to the syringe, then turn the syringe valve to “Syringe Injection position” and prime the pump.

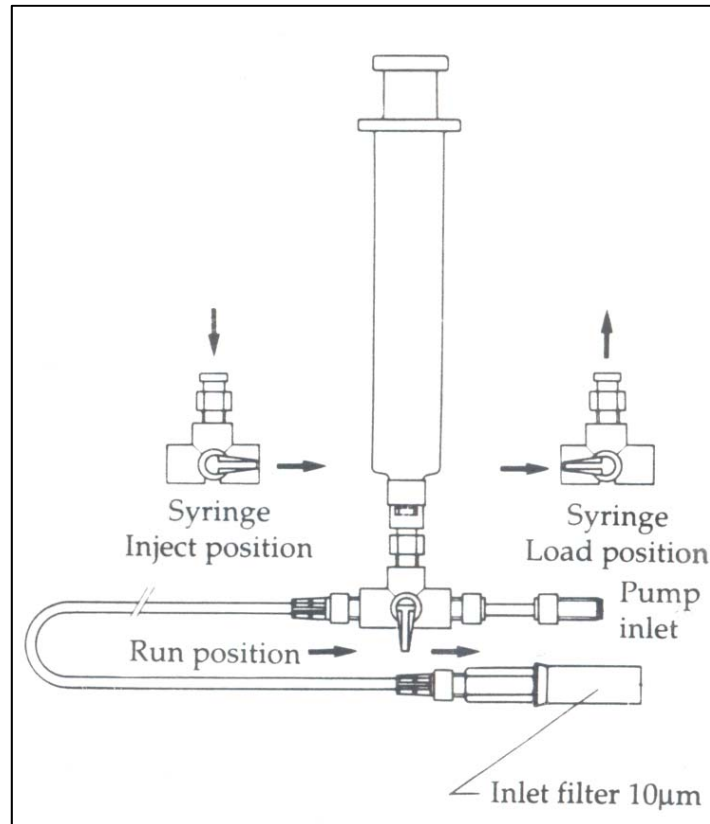


Figure 2-3: Syringe between the Pump and Fuel Tank  
Source: Gilson 305 Piston Pump User's Guide

### 2.1.2 Fuel/Air Vaporizer

This section was mainly composed of a  $\frac{3}{4}$ " stainless pipe cross and an 8400T15 cartridge heater. After the fuel and air were sent to this section, they were mixed and heated in the pipe cross, and vaporized by the cartridge heater, which provides maximum 400W heat. This heater has an internal temperature sensor thus the temperature in the pipe cross can be known from the sensor reading.



### 2.1.3 Flow Reactor

After the fuel/air mixture was vaporized, it entered the flow reactor at room pressure and mixture temperature of 180C. The flow reactor consists of 2 components: (a) the flow conditioning and flame arrester section, and (b) the test section. The flow conditioning section is composed by one 6"× 6" ×1" aluminum block and three 6" × 6" ×2" aluminum blocks as shown in Figure 2-4. The first block is the transition for 0.5" pipe to 2.5" diameter hollow part of the second block. The hollow part of the second block is filled with 3/8" glass beads, forming the porous media and conditioning the flow into uniform streamline. The hollow part in third block is designed as a cone shape to reduce the flow recirculation. And the fourth block connected the flow conditioning system to the reactor. To maintain the temperature and prevent heat loss when the vaporized mixture passed through the pipe and conditioning section, BriskHeat heating tapes (Model BAST 101006 & 101008) are wrapped around these sections and covered by high temperature insulations.

The flow reactor was placed inside a radiant furnace (MELLEN EPS-240-90), which provided an environment to adjust heat loss or heat gain to the reactor. Two reactor tubes were examined, a quartz and a pyrex tube. The reactor has 1.25" inner diameter and 1.25" outer diameter. The pyrex tube is drilled with 21 holes and K-type thermocouples are inserted in to monitor the temperature in the tube. The holes are drilled in a 90 degree spiral pattern as shown in Figure 2-5. The actual position of each thermocouple in the furnace is shown in the Table 2-1.

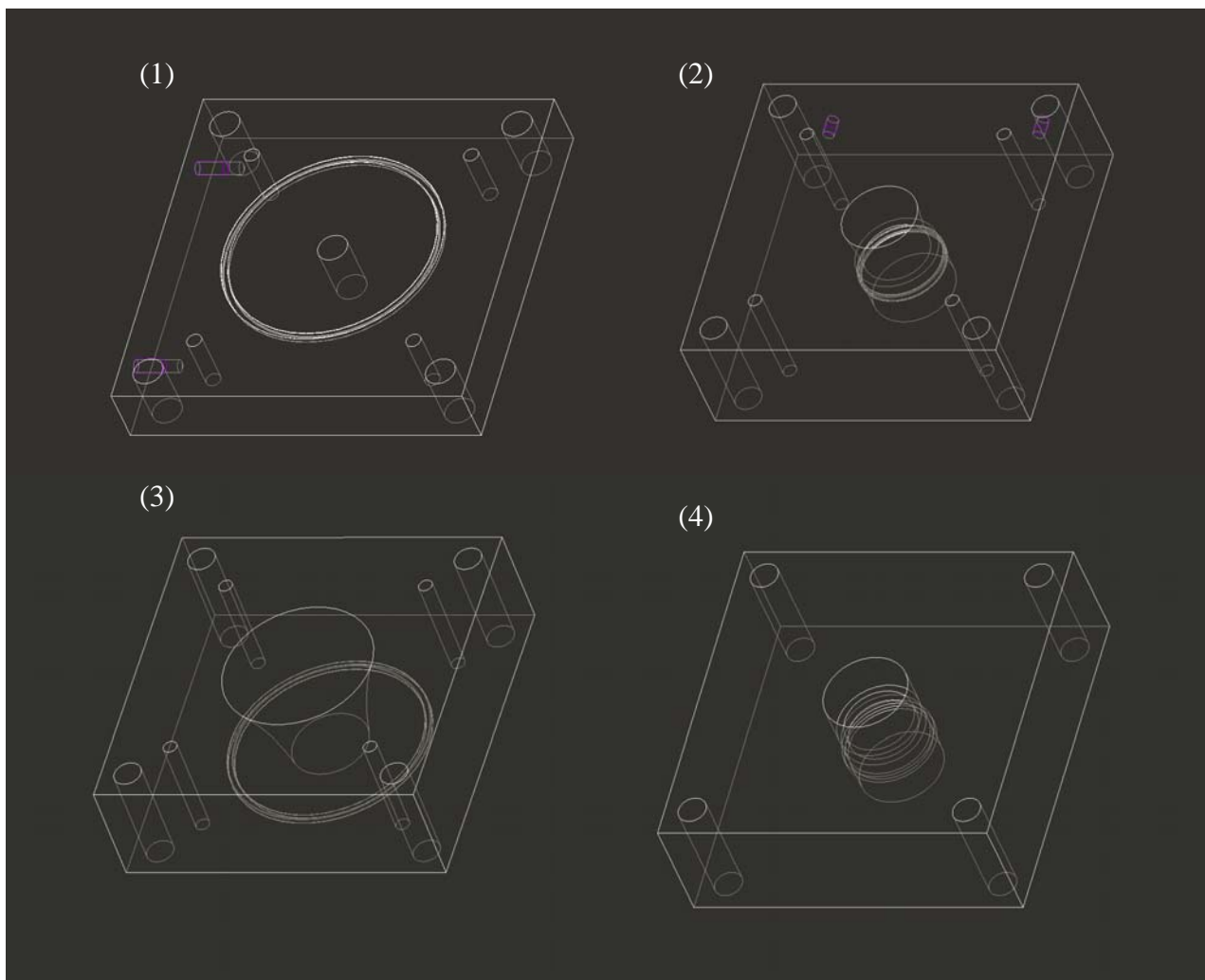


Figure 2-4: Flow Conditioning and Flame Arrester Section

Table 2-1: Thermocouple Positions in the Reactor

T.C. No.	1	2	3	4	5	6	7	8	9	10	11	12	13	14	15	16	17	18	19	20	21
x (in.)	3.75	4.75	5.75	6.75	7.75	8.75	9.75	10.75	11.75	12.75	13.75	14.75	15.75	16.75	17.75	18.75	19.75	20.75	21.75	22.75	23.75

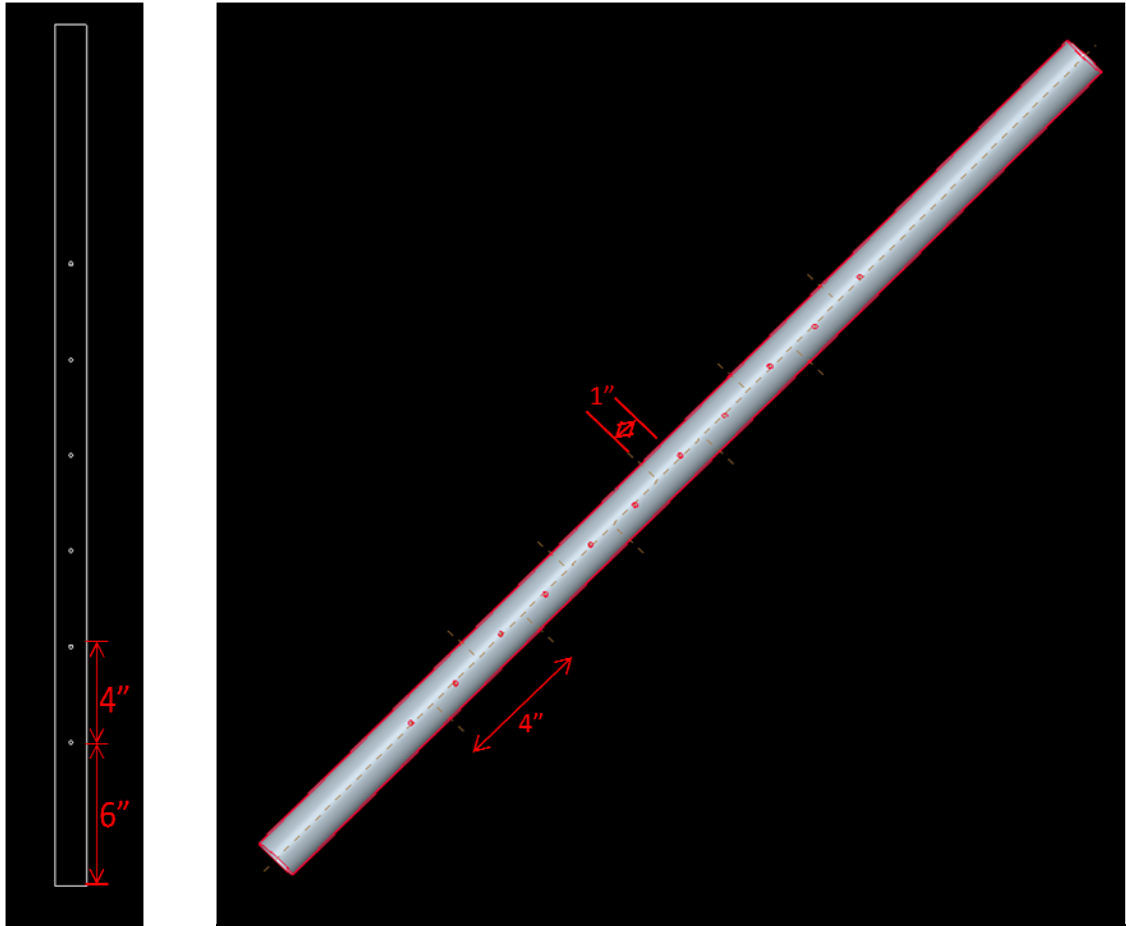


Figure 2-5: Drilled Reactor Tube

#### 2.1.4 Exhaust Burn-off

Exhaust burn-off section is crucial because of the safety issue. It burns the leftover fuel instead of letting it escape in the lab. The exhaust burn-off section is connected right after the reactor with an ID: 1.6", OD: 1.9", length: 1.5" pipe nipple. It is a 90 degree elbow filled with 3/32" diameter steel beads (Figure 2-6 & Table 2-2). An ignitor was placed at the top of the elbow exit, to burn off the unburnt mixture (Figure 2-7).

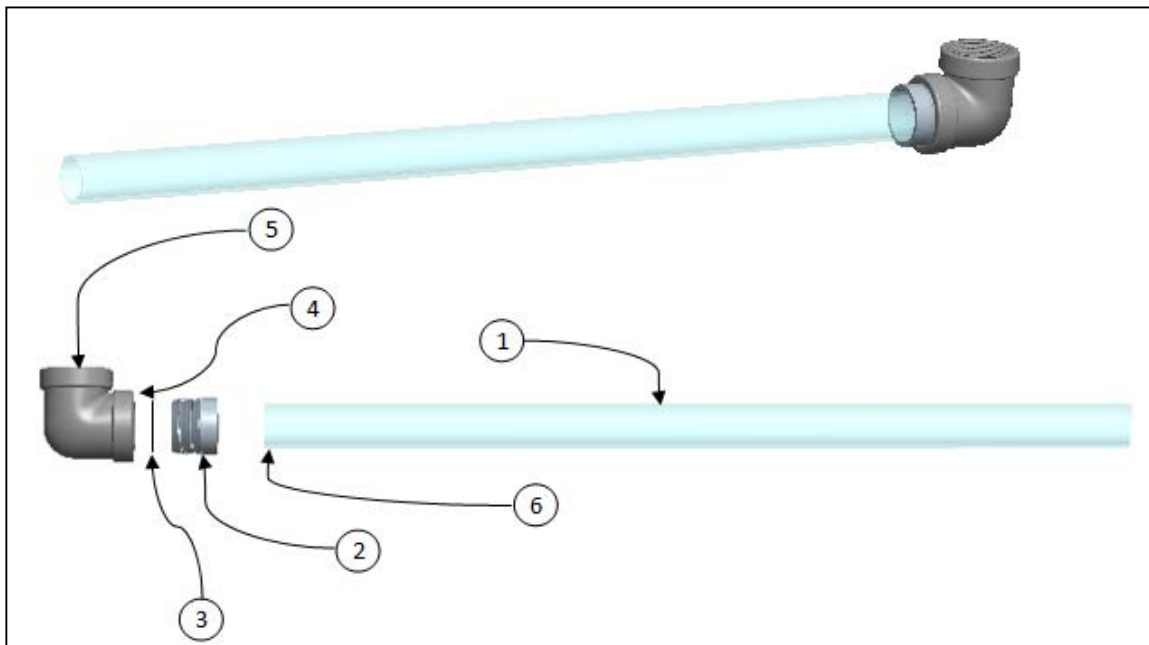


Figure 2-6: The Exhaust Burn-off Section

Table 2-2: Description of the Exhaust Burn-off Section

Item	Brief Description	
1	Reactor Tube	ID: 1.25" OD: 1.5"
2	Pipe Nipple	ID: 1.6" OD: 1.9" Length: 1.5"
3	Wire Screen	
4	90° Elbow	1.5" NPT
5	Steal Beads	3/32" Diameter 1020 Carbon Steel
6	High Temperature Sealant	Withstands temperatures up to 1100°C



Figure 2-7: Fuel Burn Off at the Reactor Exit.

### 2.1.5 Mass Flow Meter Calibration

An AALBORG CFM47 mass flow meter with a manufacturer specified accuracy was acquired in 2010 and used as lab standard to calibrate AALBORG AFM2600 mass flow meter. It can be seen that the AFM2600 indicates higher flow rate when the actual flow rate is lower than 2L/min.; and lower flow rate when the actual flow rate is higher than 2 L/min. Using second order relation, the fit can be obtained as  $y = 0.0285x^2 + 0.3752x + 1.2983$ . The random error between the data and this fit (error of the fit) is 0.235; the random uncertainty about the fit is 0.086. Therefore the second order polynomial fit can be stated at 95% confidence as  $y = 0.0285x^2 + 0.3752x + 1.2983 \pm 0.086$  L/min. The curve is plotted below with its 95% confidence interval as shown in Figure 2-8.

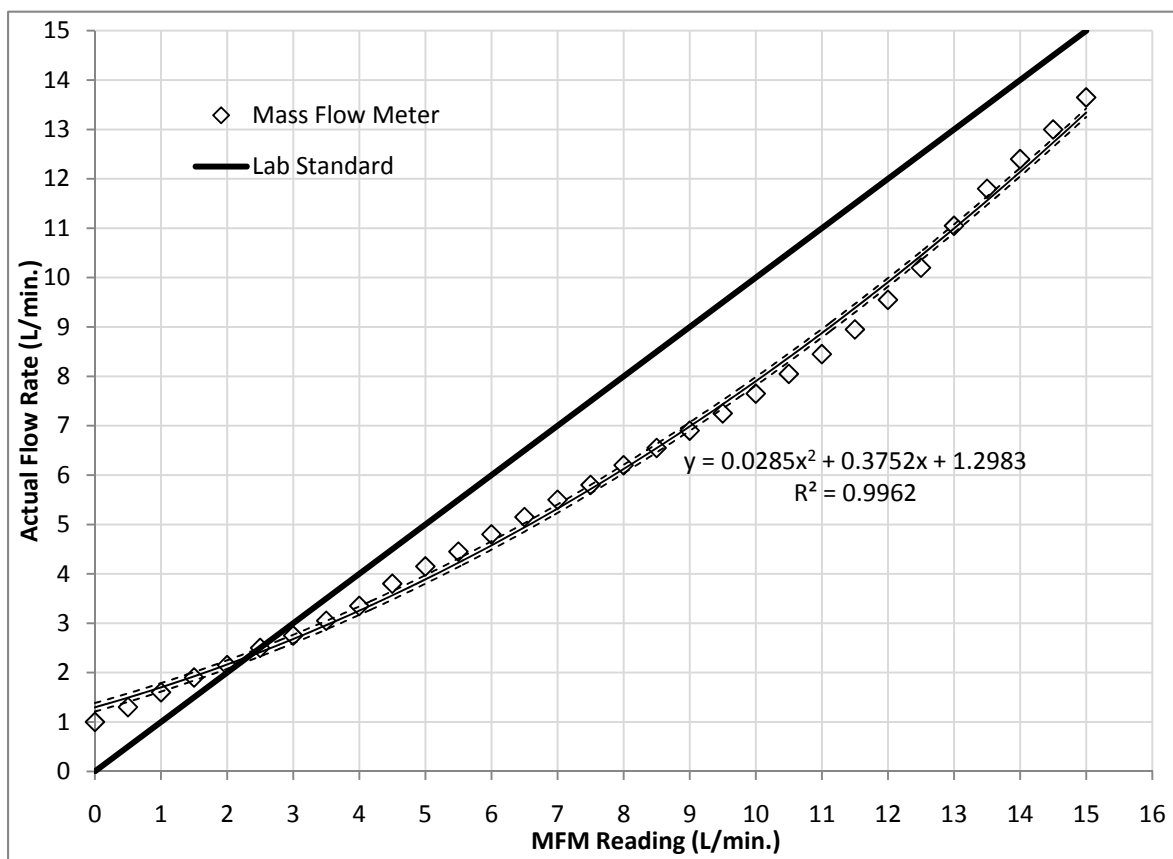


Figure 2-8: AFM2600 Mass Flow Meter Calibration

## 2.2 Experimental Procedure

Prior to turning on the experimental setup, the fuel should be prepared. Four fuels were tested in the experiment: PRF0, PRF65, PRF85, and PRF100. PRF stands for Primary Reference Fuels, including isooctane, n-heptane and mixtures of these two fuels. The numbers after PRF is the ratio of isooctane in the fuel by volume (Table 2-3). For instance, PRF100 is pure isooctane; PRF65 is the fuel that contains 65% isooctane and 35% n-heptane by volume. As mentioned in Section 1.1, this number also represents the octane number of the fuel.

Table 2-3: Fuel Composition

PRF	0	65	85	100
Octane Number	0	65	85	100
Isooctane (by volume)	0%	65%	15%	100%
n-heptane (by volume)	100%	35%	85%	0%

To start with, the cartridge heater and heating tapes were turned on to 40% - 50%. This process usually took about 2 to 3 hours to heat the air flow at the entrance of the reactor to 150C. Once the mixture reached 150C, the furnace was turned on and the temperature was set to 345C. After the furnace temperature stabilized at 345C and air flow temperature at the entrance of the reactor reached 180C, the exhaust burn-off ignitor is turned on and then fuel started being fed. The position of the cool flame was greatly influenced by the surface condition of the tube. To obtain reproducible results in a new tube it was necessary to pass the mixture through the reactor for several hours (Barusch et al., 1951).

Experiments were performed following a strict start-up procedure when any heating system is turned on. First, experiment conductor wore lab coat and goggle for

safety; fire extinguisher is prepared in case of any hazardous situation. Second, if not ready, the valves between fuel tank and pump should be closed; the pump should not be feeding until the air flow temperature at the entrance of the reactor reached 180C. Third, it was necessary to wait until the reactor outlet reaches 100 C before pumping fuel so that there would be no condensation at the reactor outlet. Last, all the electrical heating system was plugged on a socket, so it is convenient to turn off the heating system by turning of this central socket if mass smoke or large fire occurred.

After the experiment was done, stop feeding the fuel but let the system run several minutes before turning off the heating systems. This would make sure the mixture in the pipe being pushed out and burned at the outlet. Finally, turn off the heating tapes, outlet ignitor, and furnace.

### **2.3 Data Acquisition and Arrangement**

There were totally 26 thermocouples in the experimental setup. In addition to 21 thermocouples introduced in section 2.1.3, there were 5 thermocouples monitoring the heating system: cartridge heater, flow conditioning block inlet, flow conditioning outlet, furnace and exhaust burn-off outlet. These thermocouples were connected to OMEGA OMB-DAQ-56 data acquisition board and OMB-PDQ2 expansion board. The boards are connected to the laptop and DASYLab software was used to read and save the temperature that had been measured. The DasyLab interface is shown as Figure 2-9.

There were 26 digital meters displaying the measured temperatures of each thermocouple. As shown in Figure 2-9, the five digital meters at the upper left was showing the temperature of cartridge heater, flow conditioning block inlet, flow conditioning outlet, furnace and exhaust burn-off outlet respectively. The reactor thermocouples' digital meter windows are minimized; instead, two charts at the bottom were showing the temperature depending on time. Thermocouples 1 to 10 were shown in

the left chart and 11 to 21 were shown in the right chart. Different thermocouples were labeled by different colors so that it is easier to observe the temperature rise at each thermocouple. Since DasyLab did not save the chart data, the thermocouple data were saved as ASC files and read by Microsoft Excel. An example of the saved Excel data is shown in Figure 2-10. Because the time interval of each datum was 1.68 second, there were usually more than thousands of data in the file. It is a good idea to take snapshots while the experiment performer sees the temperature rise from the charts, and then go back to look up the temperatures at that time.

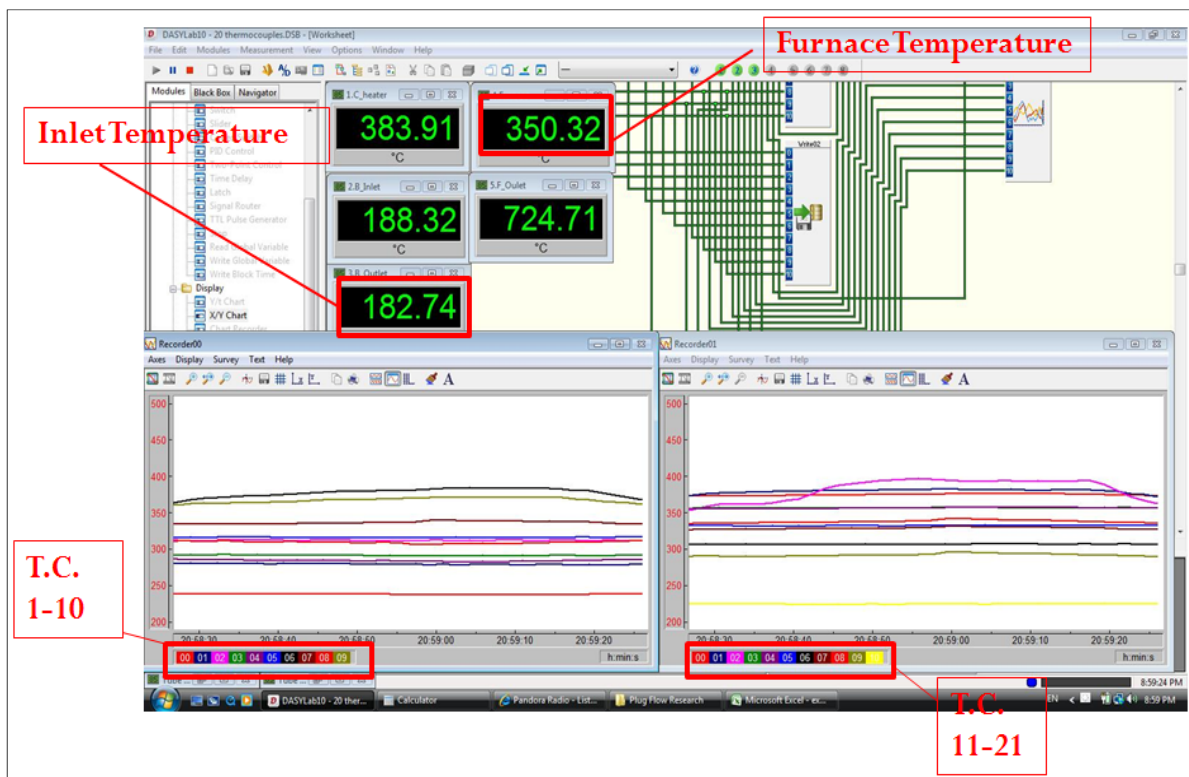


Figure 2-9: Interface of DasyLab



The screenshot shows an Excel spreadsheet titled 'TEST20100626\_tube1-10\_PRRF.ASC'. The data is organized as follows:

- Row 1:** DASLab - V 10.00.01
- Row 2:** Worksheet name: 20 thermocouples
- Row 3:** Recording date : 6/26/2010, 7:37:43 PM
- Row 4:** Block length : 1
- Row 5:** Delta : 1.681 sec
- Row 6:** Number of channels : 10
- Row 7:** Measurem Write 0 [V Write 1 [V Write 2 [V Write 3 [V Write 4 [V Write 5 [V Write 6 [V Write 7 [V Write 8 [V Write 9 [V Write 10 [V Write 11 [V Write 12 [V Write 13 [V Write 14 [V Write 15 [V Write 16 [V Write 17 [V Write 18 [V Write 19 [V Write 20 [V
- Rows 8-40:** Data rows containing time (e.g., 00:07.9, 00:09.6, 00:11.3, etc.) and temperature values for 20 channels (V1 to V20).

Figure 2-10: Temperature Data Saved in Excel File

Another issue to mention is that the 21 thermocouples inserted in the reactor were placed at different axial locations and with varying azimuthal angles that repeat its location every four thermocouples. As shown in Figures 2-11 and 2-12, no matter the furnace was turned off or fixed at 345C, in every four thermocouples, and the 2<sup>nd</sup> and 3<sup>rd</sup> thermocouples have higher temperature than the 1<sup>st</sup> and 4<sup>th</sup> thermocouples. Therefore, it was meaningless to compare the temperature of different thermocouples; instead, one should notice the temperature change in one thermocouple depending on time. For example, as shown in Figure 2-13, when the PRF65 flow velocity is 0.1 m/s, equivalence ratio is 1, and taking one minute interval, one can find out that temperature oscillates at the 7<sup>th</sup> thermocouple and 13<sup>th</sup> thermocouple, and had 40 and 50 degree jump respectively. This stands for the cool flame appeared at 9.75" and 15.75" from the reactor inlet.

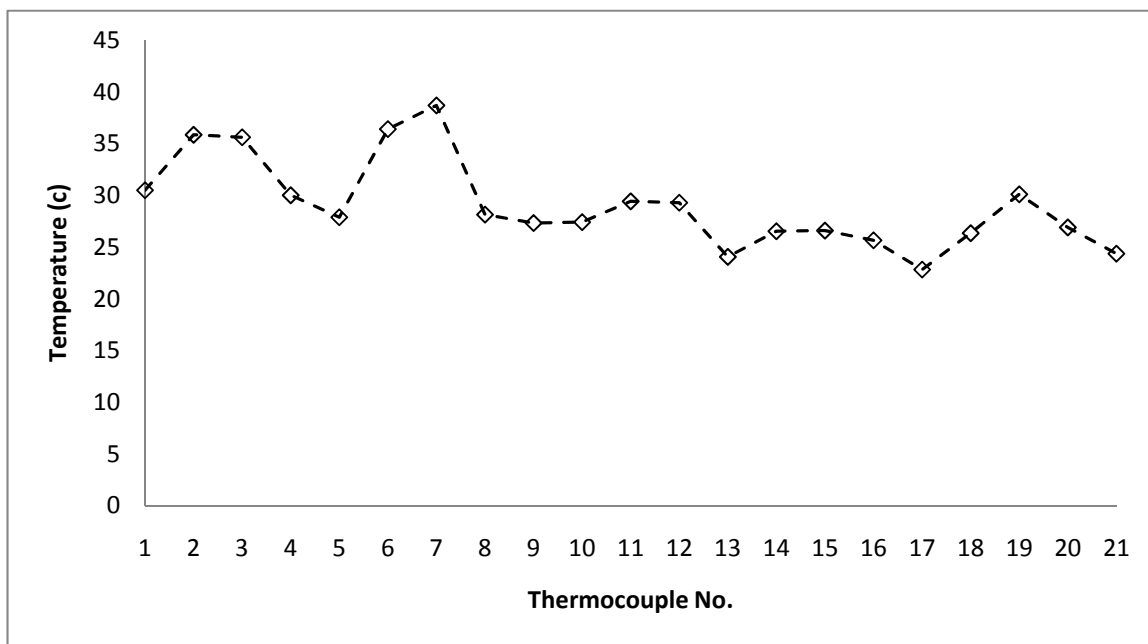


Figure 2-11: Reactor Thermocouples at Room Temperature

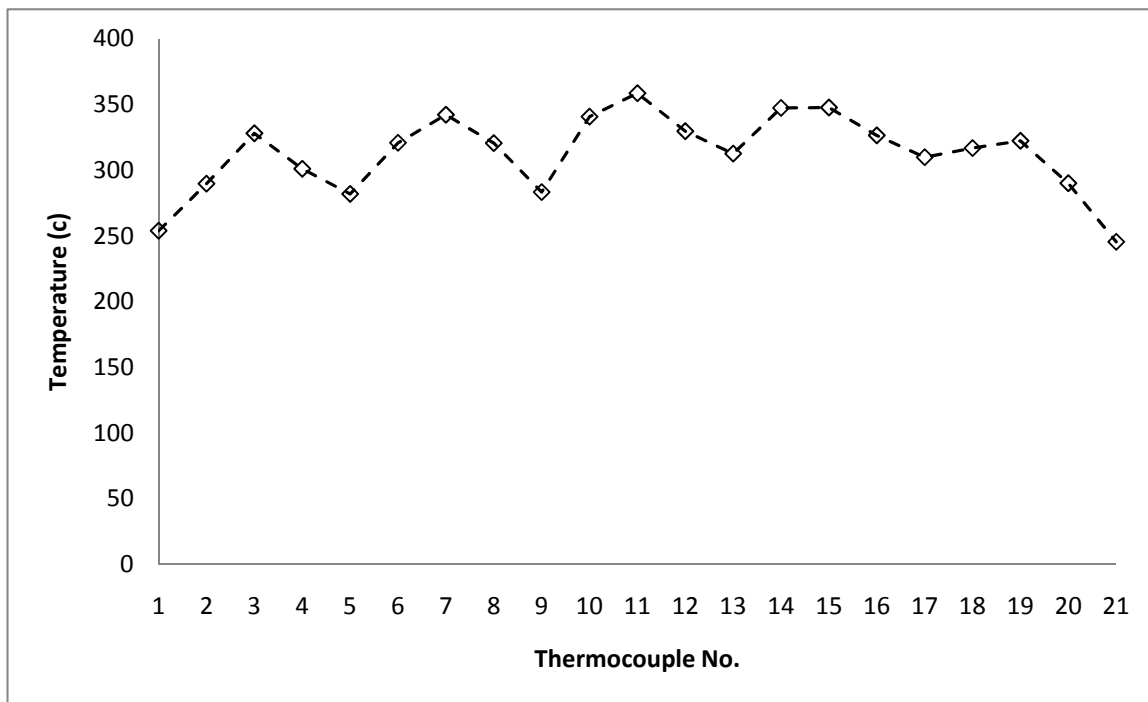


Figure 2-12: Reactor Thermocouples when Furnace Was Set to 345C

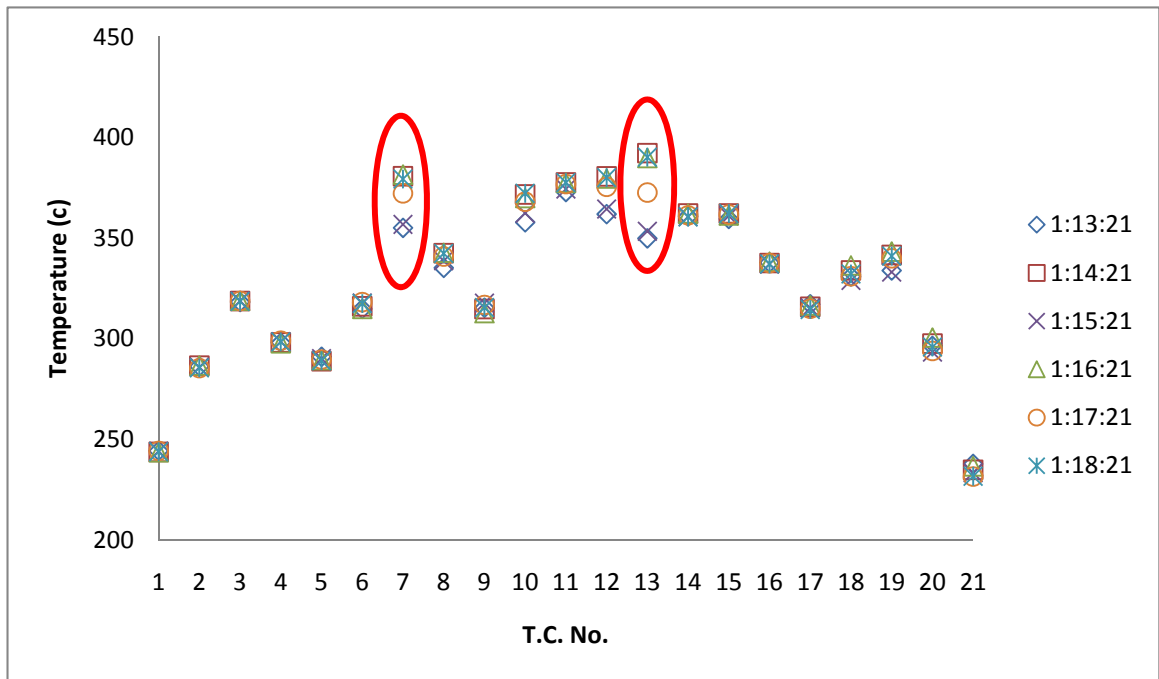


Figure 2-13: Temperature Oscillation at Each Thermocouple Taking One Minute time Interval

## CHAPTER 3: RESULT AND DISCUSSION

### **3.1 Illumination and Temperature Rise in**

#### **Different Material Reactors**

Two different material reactors had been tested in this experiment: quartz and pyrex tubes. Before inserting the thermocouples, the results were expected to see light emission accompanying with cool flame. In the past, the detection of this radiation, with the aid of photomultipliers, has been used as a diagnostic of cool-flame formation (Outlet et al., 1950 & Lucquin et al., 1958). Hence, the first goal of the experiment was to observe the light emission in the reactor tube. To observe the faint light emission during the slow combustion, a prism was located on the reactor outlet and a camera was used to record the visual situation in the reactor through the prism. There was also a K-type thermocouple probe closely attached to the reactor to measure the temperature of outer wall of the reactor at 13" from the reactor entrance.

The experiment began with using the quartz tube. Two fuels are tested: isooctane (PRF100) and n-heptane (PRF0). In order to prevent flashback, the mixture velocity was started from a higher one to lower one gradually. The experiment started from 0.4 m/s to 0.1 m/s and equivalence ratio 1.06 isooctane (PRF100)/ air mixture velocity by a 0.1 m/s decrement. Each velocity trial ran at least 30 minutes to coat the reactor wall surface with hydrocarbon component (Barusch et al., 1951).

During the above tests, no light emission was observed so the mixture was decreased from 0.07 m/s to 0.02 m/s (Stepanskii et al., 1981) by a 0.01 m/s decrement. After finishing testing with isooctane, n-heptane was tested following above procedure. However, neither faint light nor temperature rise was observed.

Then the experiment was tested at equivalence ratio greater than 1 but smaller than 2. Using isooctane (PRF100) as fuel and fixing mixture velocity at 0.0197 m/s (Stepanskii et al., 1981), the equivalence ratio was set at 1.2, 1.5, 1.7 and 2.0 for each run.

Again, neither faint light nor temperature rise was observed even the equivalence ratio was increased. The testing matrix and results are shown in Tables 3-1 to 3-3.

The failure of the test was due to wall termination during the heterogeneous reaction. At low pressure, the predominant chain termination steps in the gaseous oxidation are heterogeneous, involving the removal at wall of chain carriers and branching agents to give inactive products. It was established that base- or salt- coated reactor vessels destroy HO<sub>2</sub> radicals efficiently but boric acid- coated vessel does not (Fish, 1968).

Table 3-1: Fixing ER=1.06, Changing Mixture Velocity (PRF0, PRF100)

Mixture Velocity (m/s)	0.4	0.3	0.2	0.1
Temperature Oscillation	×	×	×	×
Visible Light	×	×	×	×

Table 3-2: Fixing ER=1.06, Changing Mixture Velocity (PRF0, PRF100)

Mixture Velocity (m/s)	0.07	0.06	0.05	0.04	0.03	0.0197
Temperature Oscillation	×	×	×	×	×	×
Visible Light	×	×	×	×	×	×

Table 3-3: Fixing Mixture Velocity at 0.0197m/s, Changing Equivalence Ratio (PRF0, PRF100)

ER	1.2	1.5	1.7	2.0
Temperature Oscillation	×	×	×	×
Visible Light	×	×	×	×

Therefore, the reactor material was switched to pyrex, which was also known as borosilicate tube. Following the testing procedure of quartz reactor test, no visible light were observed. However, there was temperature oscillation detected by the attached thermocouple probe after a 4-hour run. At first this oscillation has a maximum rise of 500C, but after 4 minutes the temperature rose to 1400C and higher, as shown in Figure 3-1. Also, after the experiment, yellow deposits could be found on the tube wall as shown in Figure 3-2. This shows great evidence that pyrex tube did provide a better environment for combustion process. The testing condition of the success trial is shown in Table 3-1.

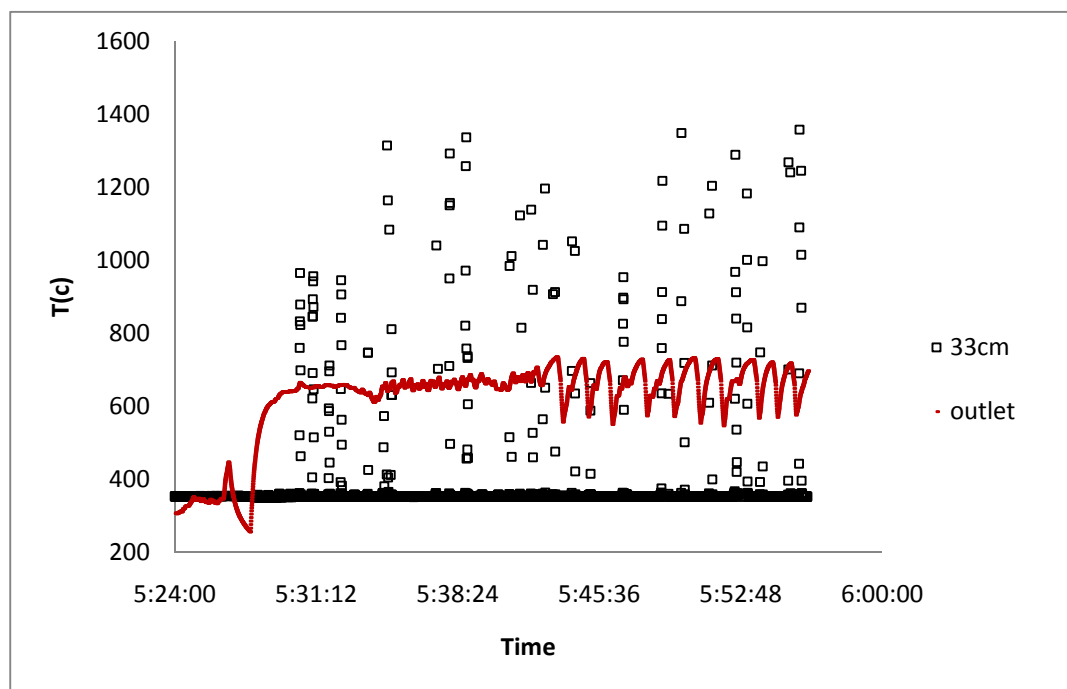


Figure 3-1: Temperature Oscillation at Middle of Reactor and Outlet

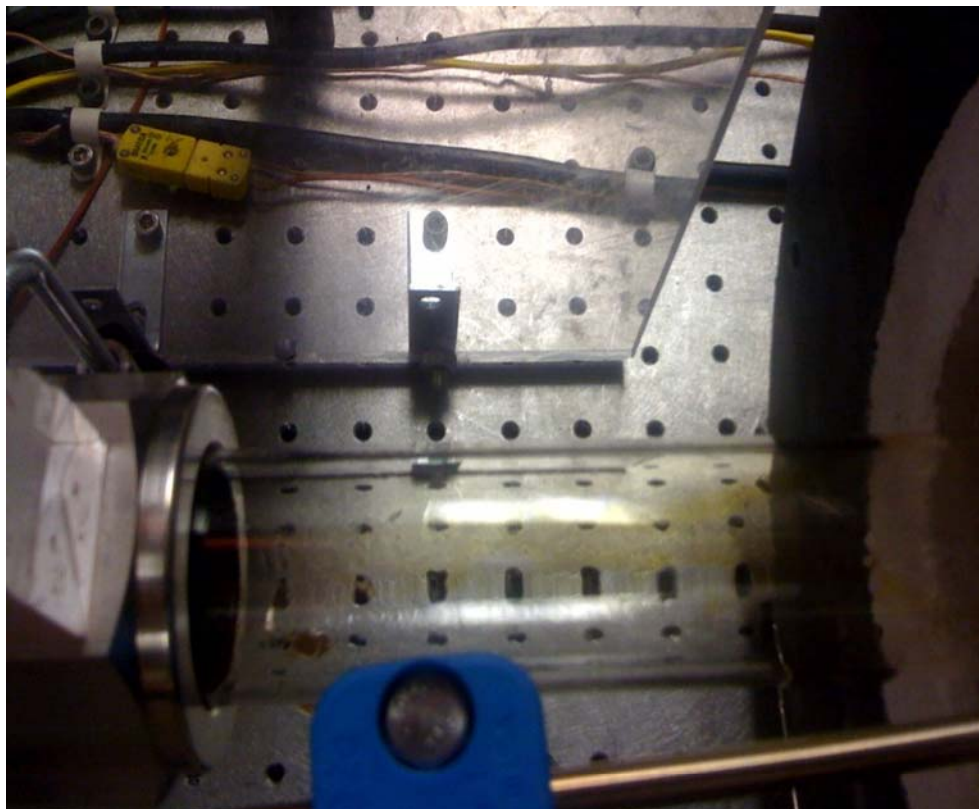


Figure 3-2: Yellow Deposits on Reactor Wall

Table 3-4: Testing Condition of the Successful Trial

Fuel	n-heptane (PRF0)
ER	0.93
Mixture Flow Speed	0.3m/s
Fuel Rate	1.19 ml/min.
Air Rate	11 l/min.
Inlet Temperature	180C
Furnace Temperature	345C

### **3.2 Suitable Conditions for the Experiment**

After knowing there was an actual combustion process in the experimental setup, the pyrex reactor with inserted K-type thermocouples was tested. In this test, the goal is to find out a suitable condition that makes the picked fuel (PRF0, PRF65, PRF85, and PRF100) work in the experimental setup. Since PRF0 was successfully tested and the temperature rise was discovered before, the experiment began with PRF65, feeding high velocity of mixture to low velocity.

In this test, the equivalence ratio was fixed at 1 but different parameters such as furnace temperature, inlet temperature and mixture velocity were adjusted in order to find the best temperature oscillation. Using PRF65, as the mixture velocity was set at 0.1 m/s, inlet temperature 182C, furnace temperature 350C, the temperature oscillations started being observed (Figures 3-3 and 3-4). As Figure 3-5 shows, the temperature rose from 355C to 380C at the 7<sup>th</sup> thermocouple, and rose from 350C to 395C at the 13<sup>th</sup> thermocouple, while the other thermocouples remained at very stable temperature. Although the 13<sup>th</sup> thermocouple has the maximum temperature rise, it is also noticeable that the 7<sup>th</sup> thermocouple was the first position where cool flame starts.

However, under the above condition but using PRF85, the temperature oscillated at the same position but disappeared after 3 minutes. Therefore, it was a good idea to turn the flow velocity slightly lower to increase the residence time in the reactor.

While the inlet temperature remained at 182C and furnace temperature 350C, turning down the mixture velocity to 0.085 m/s, more clear oscillation was observed at the 7<sup>th</sup> and 13<sup>th</sup> thermocouple, as shown in Figures 3-6 and 3-7.

If the furnace temperature was turned down to 345C under above conditions, even more clear temperature oscillations (shorter oscillation time periods) could be observed at the 7<sup>th</sup> and 13<sup>th</sup> thermocouple as shown in Figures 3-8, 3-9 and 3-10. With furnace temperature going lower, temperature oscillations disappeared. This indicated that the best condition to run this experiment was shown as Table 3-2.



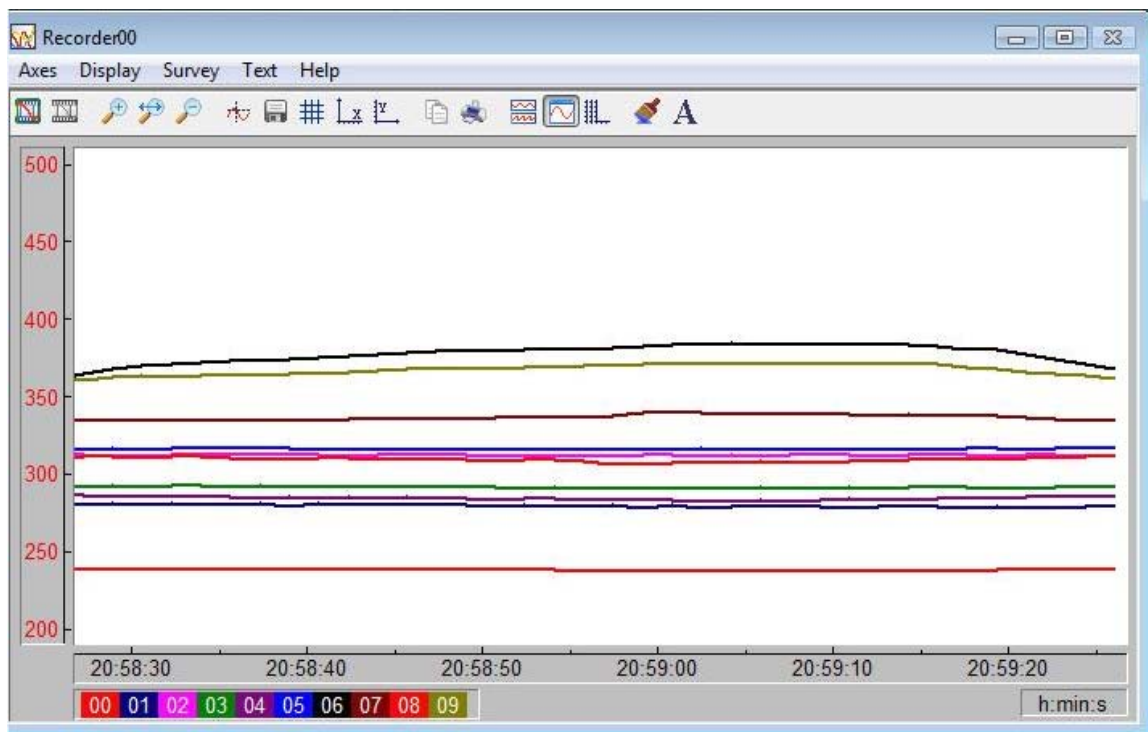


Figure 3-3: Temperature Oscillation of Thermocouple 1-10 ( $v= 0.1$  m/s, Inlet Temperature 182C, Furnace Temperature 350C.)

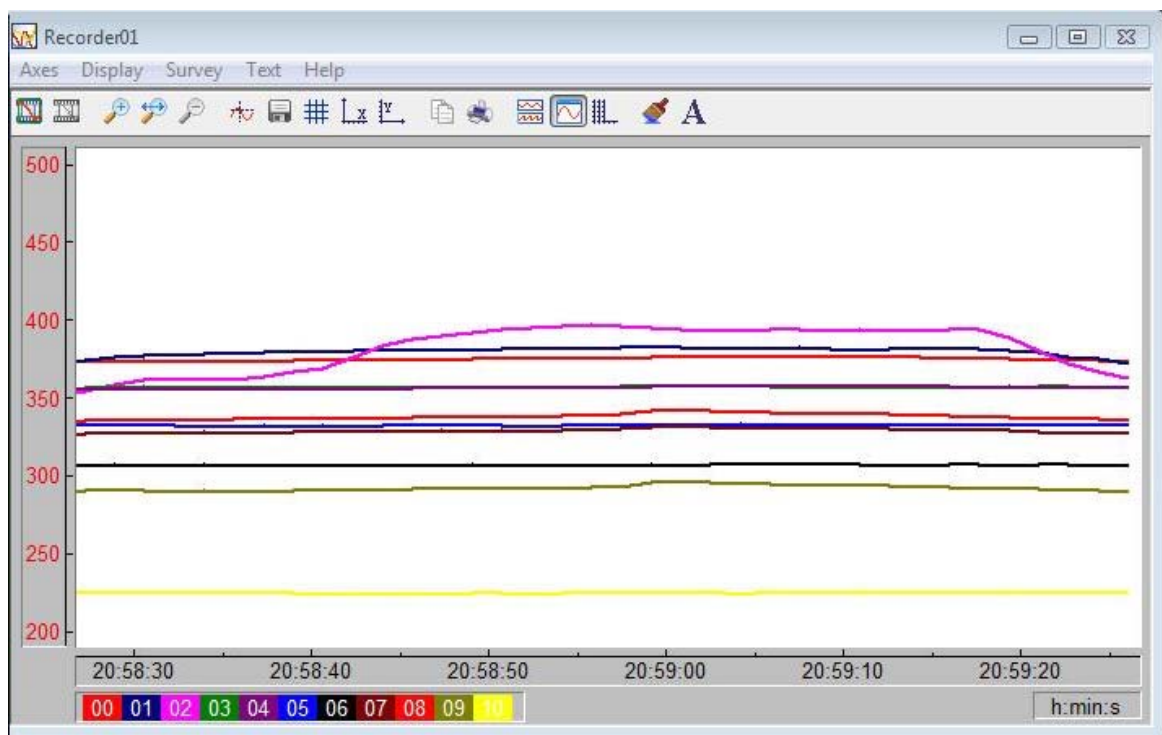


Figure 3-4: Temperature Oscillation of Thermocouple 11-21 ( $v= 0.1$  m/s, Inlet Temperature 182C, Furnace Temperature 350C.)

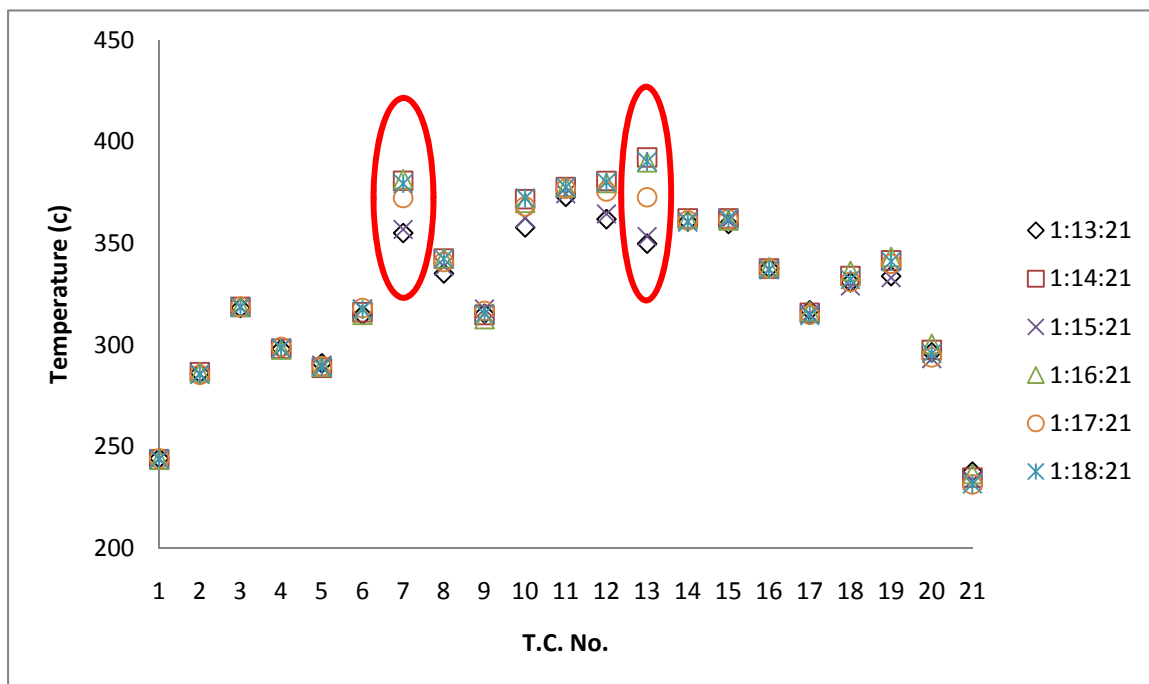


Figure 3-5: Temperature Oscillation in the Reactor Per Minute ( $v = 0.1$  m/s, Inlet Temperature 182C, Furnace Temperature 350C.)

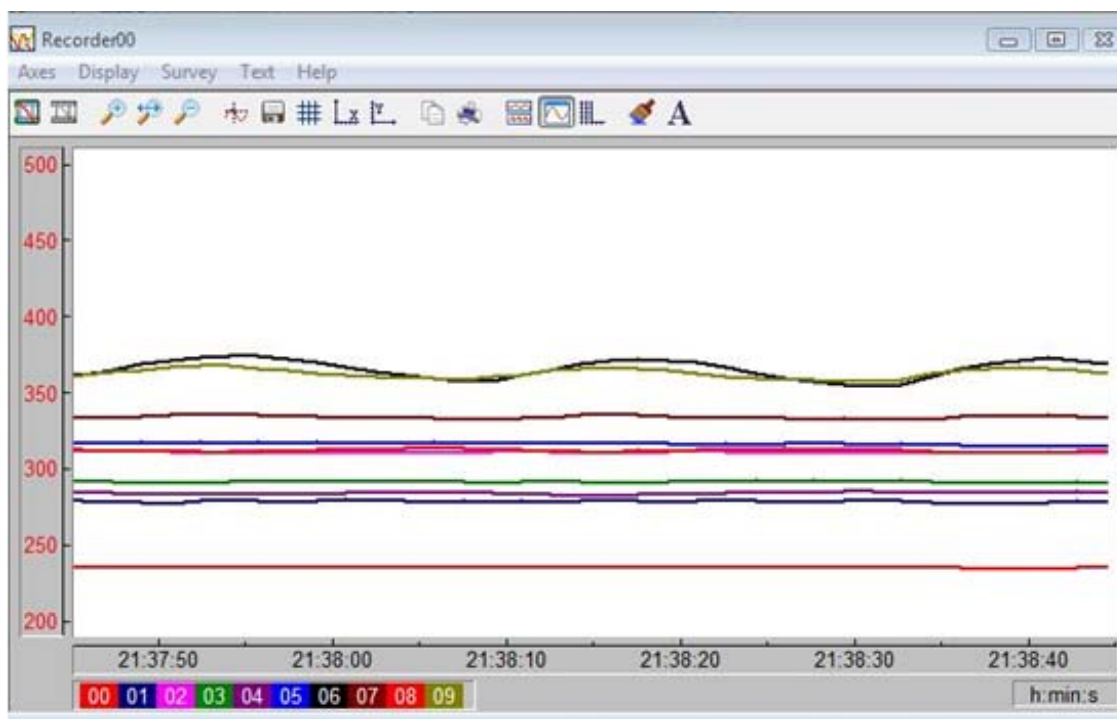


Figure 3-6: Temperature Oscillation of Thermocouple 1-10 ( $v = 0.085$  m/s, Inlet Temperature 182C, Furnace Temperature 350C.)

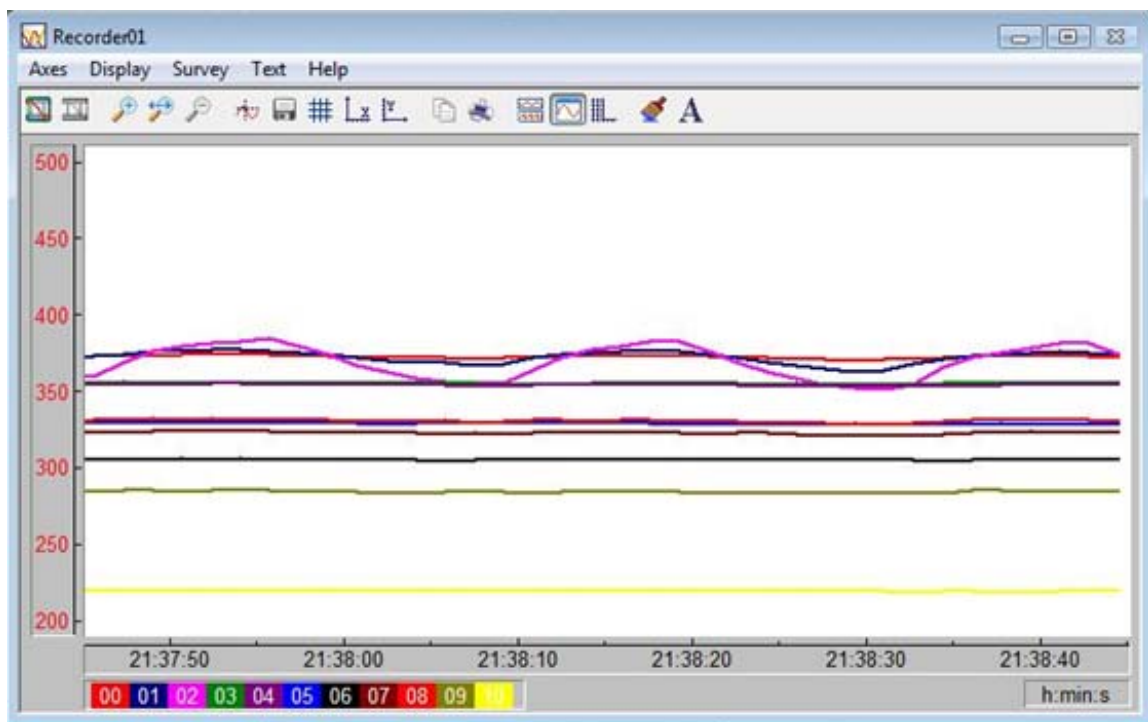


Figure 3-7: Temperature Oscillation of Thermocouple 11-21 ( $v= 0.085$  m/s, Inlet Temperature 182C, Furnace Temperature 350C.)

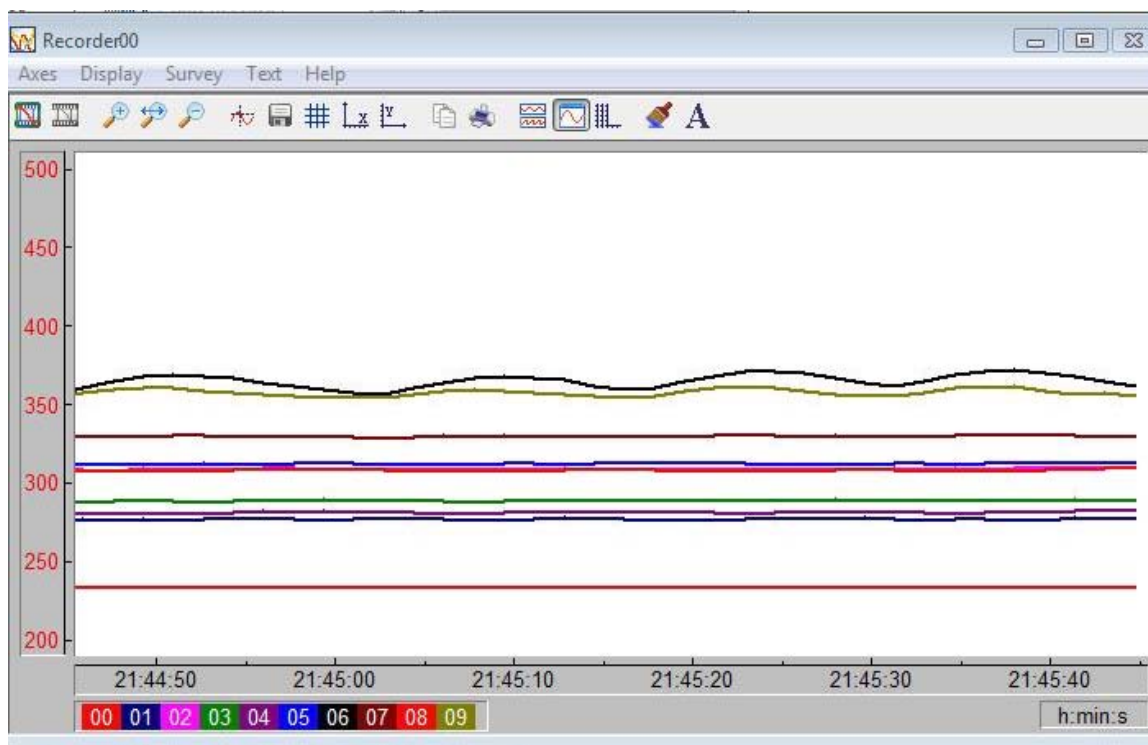


Figure 3-8: Temperature Oscillation of Thermocouple 1-10 ( $v= 0.085$  m/s, Inlet Temperature 182C, Furnace Temperature 345C.)

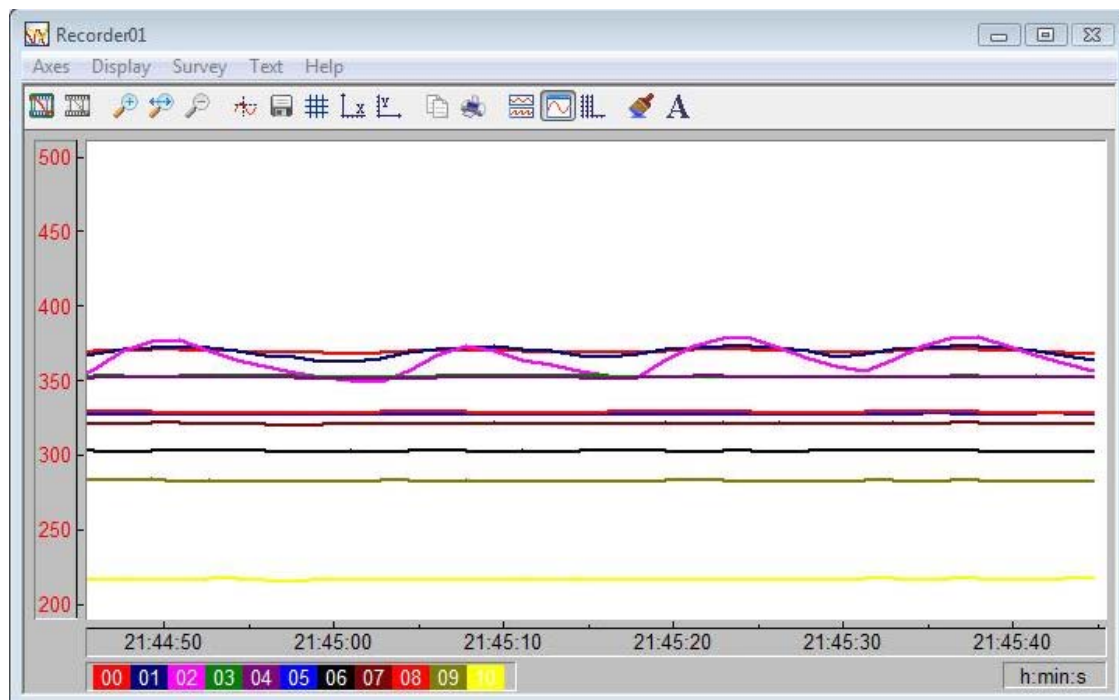


Figure 3-9: Temperature Oscillation of Thermocouple 11-21 ( $v= 0.085$  m/s, Inlet Temperature 182C, Furnace Temperature 345C.)

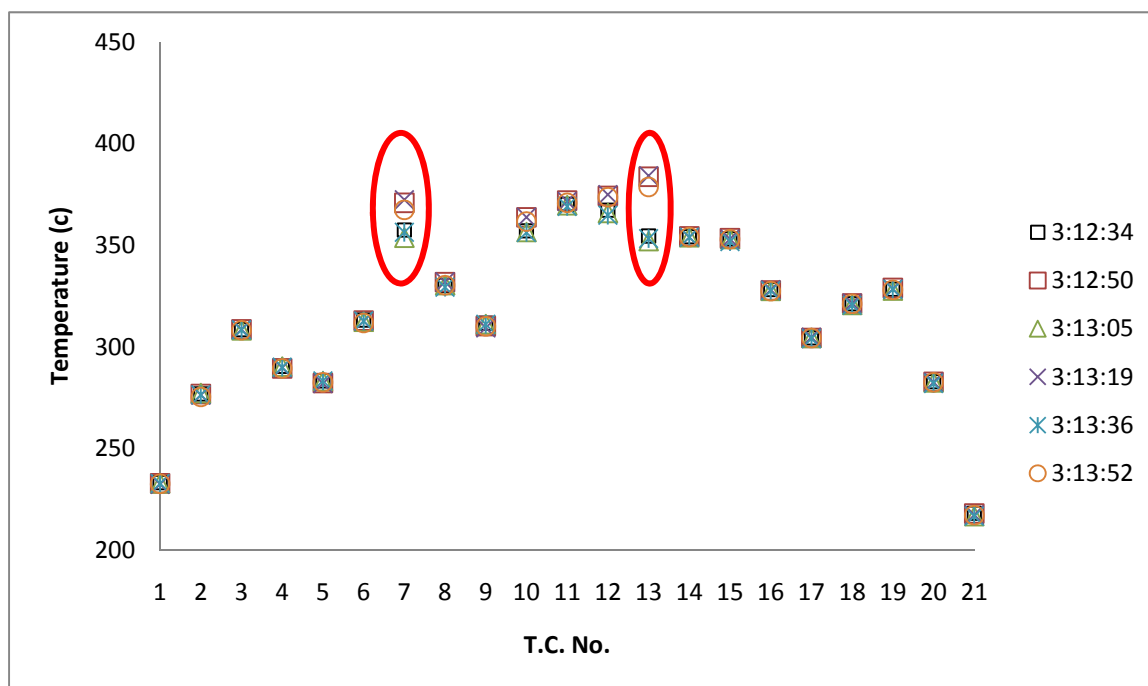


Figure 3-10: Temperature Oscillation in the Reactor Every 15 Seconds ( $v= 0.085$  m/s, Inlet Temperature 182C, Furnace Temperature 345C.)

Table 3-5: Testing Condition of the Most Clear Temperature Oscillation

ER	1
Mixture Flow Speed	0.085m/s
Fuel Rate	0.383 ml/min.
Air Rate	3.12 l/min.
Inlet Temperature	182C
Furnace Temperature	345C

Following the above experimental condition but gradually decreasing the flow velocity to 0.05 m/s, the temperature oscillated but less obvious as shown in Figures 3-11 and 3-12. From Figures 3-13 and 3-14, one can found that the temperature at 13<sup>th</sup> thermocouple did not jump and the maximum temperature position shifted to the 8<sup>th</sup> thermocouple. Also, the maximum temperature change range was averagely 25C degree, almost half of it when the flow velocity was 0.085 m/s. As the flow velocity went to 0.04 m/s, the temperature oscillation disappeared. The conditions also worked for PRF0 and PRF85 but not for PRF100. PRF100 was tested by changing many other parameters but failed to derive the ignition.

From the result above, it can be tell that for PRF65, a better result can be found when the equivalence ratio is 1, the mixture velocity is 0.085m/s, the inlet temperature is about 180C and furnace temperature at 345C.

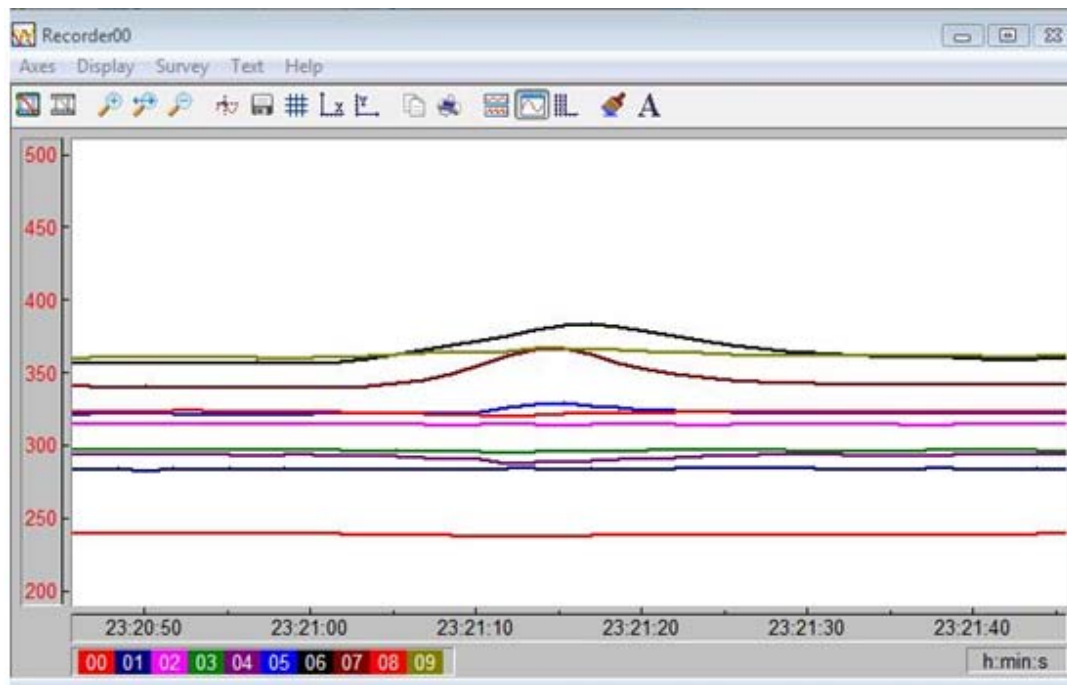


Figure 3-11: Temperature Oscillation of Thermocouple 1-10 ( $v= 0.05$  m/s, Inlet Temperature 182C, Furnace Temperature 345C.)

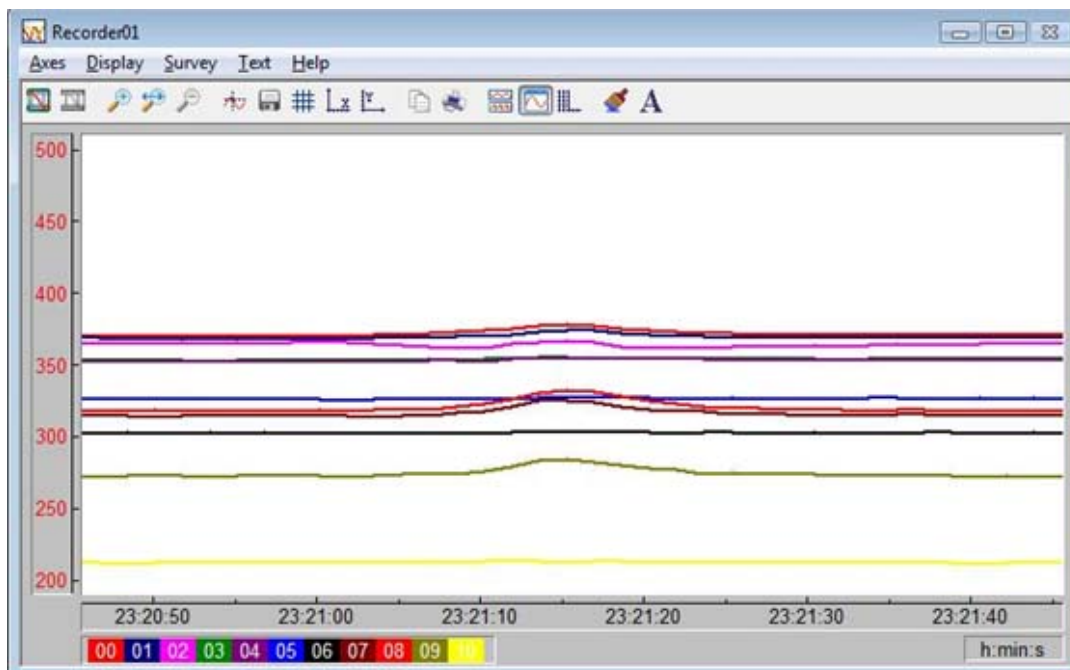


Figure 3-12: Temperature Oscillation of Thermocouple 11-21 ( $v= 0.05$  m/s, Inlet Temperature 182C, Furnace Temperature 345C.)

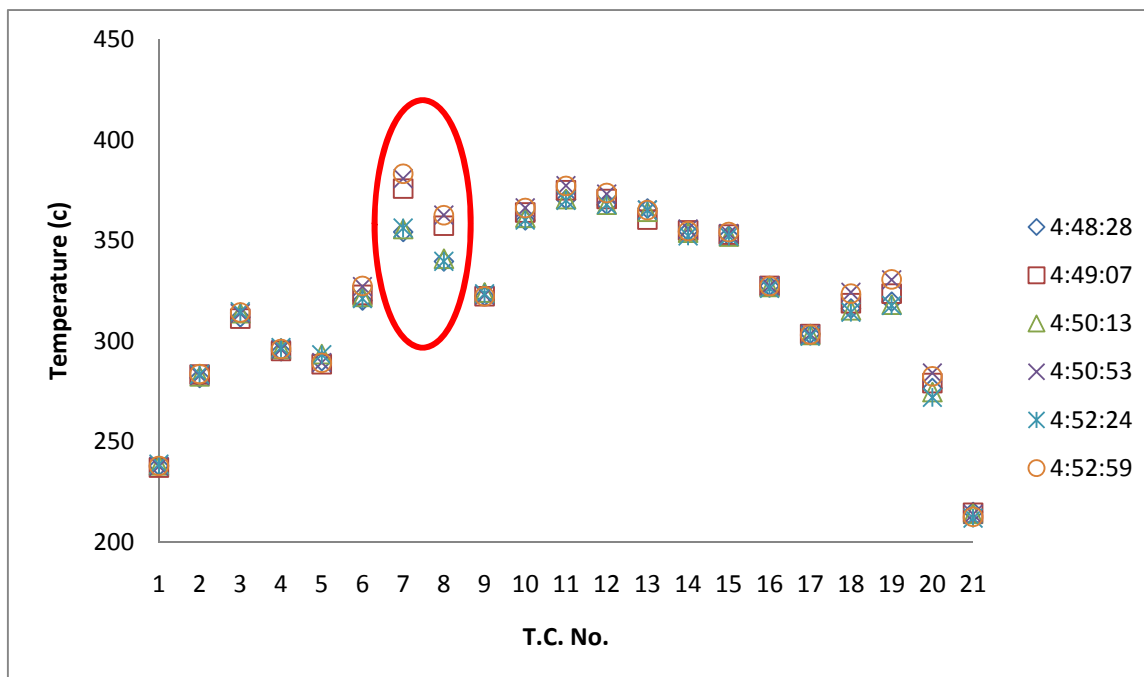


Figure 3-13: Temperature Oscillation in the Reactor ( $v = 0.05$  m/s, Inlet Temperature 182C, Furnace Temperature 345C.)

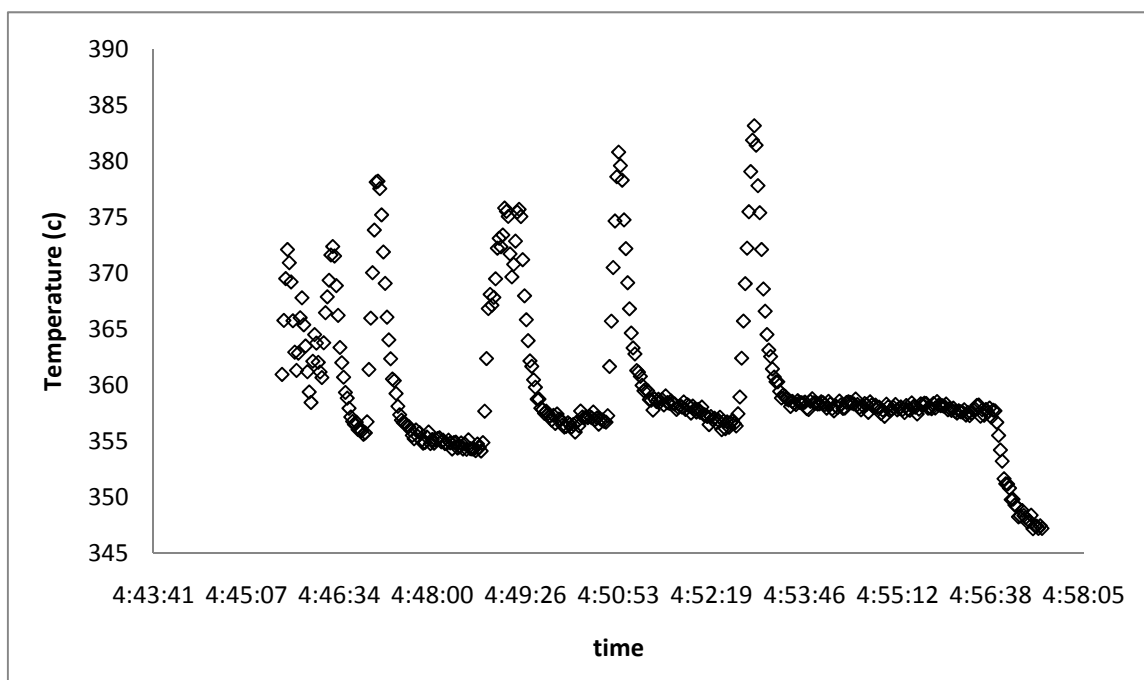


Figure 3-14: Temperature Oscillation at the 8<sup>th</sup> Thermocouple ( $v = 0.05$  m/s, Inlet Temperature 182C, Furnace Temperature 345C.)

### **3.3 Comparison and Discussions of the Three Trials**

After finding out the suitable conditions of this experiment, three runs were performed and the results were compared. All the results are shown in Figures 3-15 to 3-20. As Figure 3-15 shows, there are two y-axes: the dimensionless length on the left and the temperature on the right y-axis. The “x” in the figure indicates the position where initial cool flame appeared, and the red bar stands for the temperature jump in that position.

Since there was more than one position that the temperature had oscillated, the two remarkable oscillation positions were compared: one is the initial cool flame position, where was the closest position from the reactor inlet that the temperature jumped more than 10 degrees. The other one is the maximum temperature oscillation position, where the temperature had the largest rise in the reactor. For example, as shown in Figures 15 and 16, using PRF0 as fuel, one can know that the first position that cool flame had been discovered was at the 0.242 of the reactor length from the entrance, and the temperature jumped from 328C to 341C averagely. Its largest temperature rise was at the 0.495 of the reactor length, and temperature rose from 342C to 414C. For PRF65, the first position that cool flame had been discovered was at the 0.410 of the reactor length, and at that position the temperature rose from 358C to 375C. The largest temperature rise was at 0.663 of the reactor length, and temperature rose from 353C to 383C and so on.

From Figures 3-15, 3-17 and 3-19, one finds that for all the trials, the initial cool flame positions were the same except PRF85 in the third trial, which the initial cool flame position was at 0.873 instead of 0.915 from trial 1 and 2. In other words, in trial 3, the cool flame started to be discovered at 1” prior to the initial cool flame position of trial 2 and trial 3. This can be interpreted as the cool flame propagated upstream slightly. The temperature rising ranges were similar but not exactly the same.

This indicates that the initial cool flame was reproducible in certain position; however, the temperature rising ranges were not be able to control.



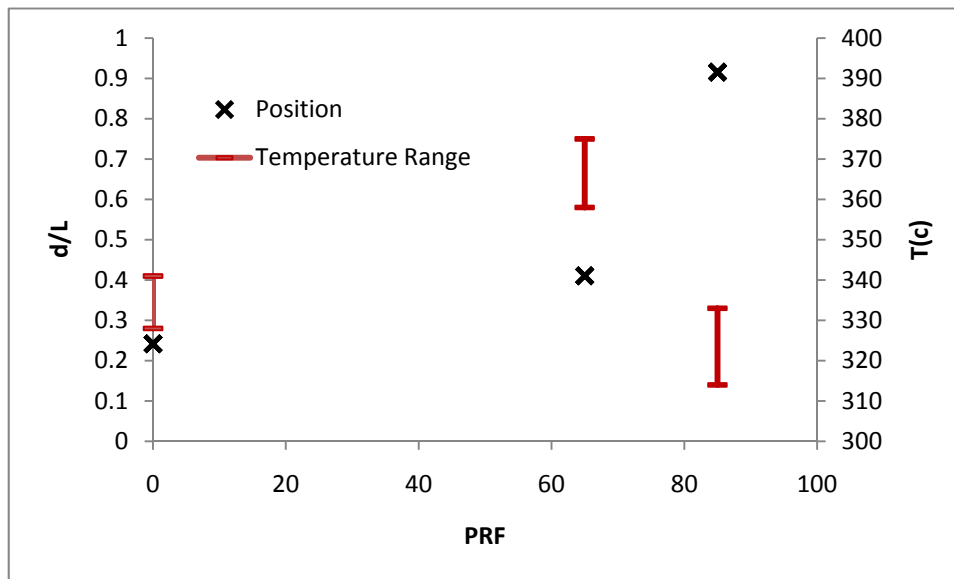


Figure 3-15: The Initial Cool Flame Positions and Temperature Rise of Trial #1

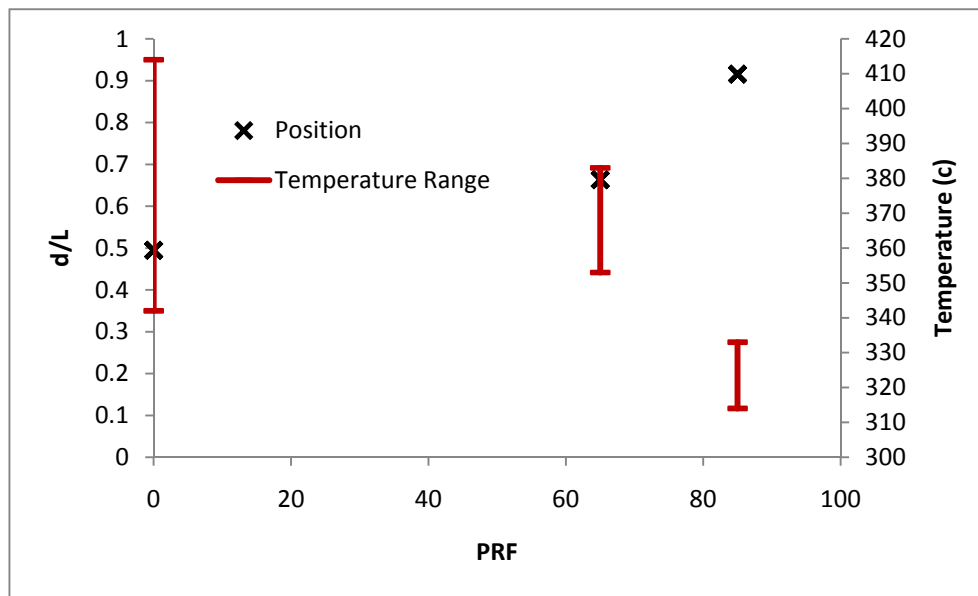


Figure 3-16: The Maximum Temperature Change Positions and Range of Trial #1

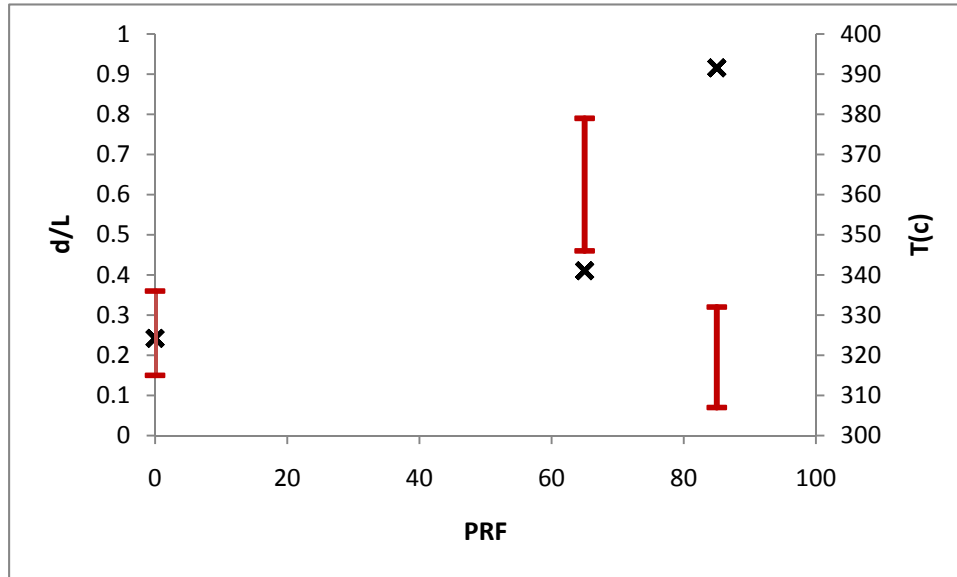


Figure 3-17: The Initial Cool Flame Positions and Temperature Rise of Trial #2

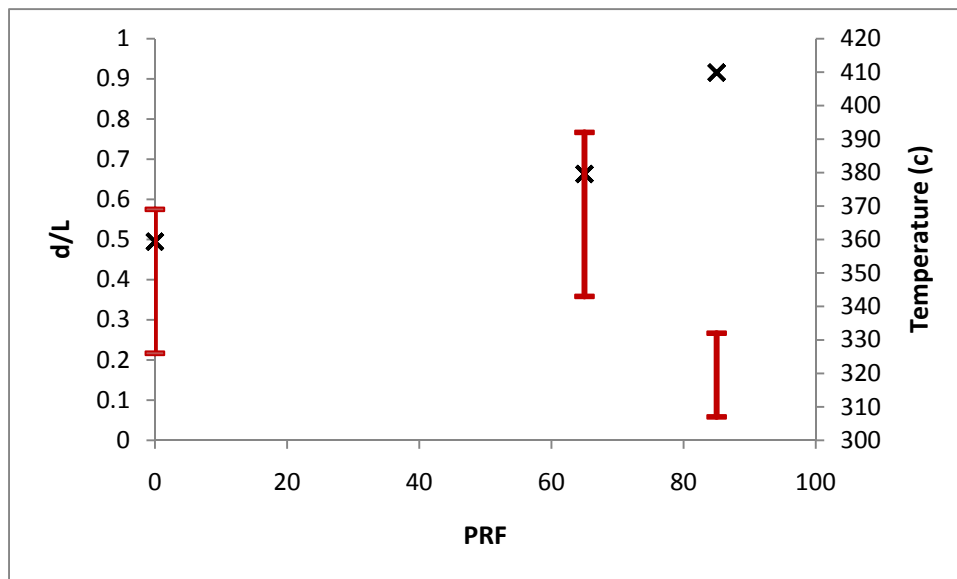


Figure 3-18: The Maximum Temperature Change Positions and Range of Trial #2

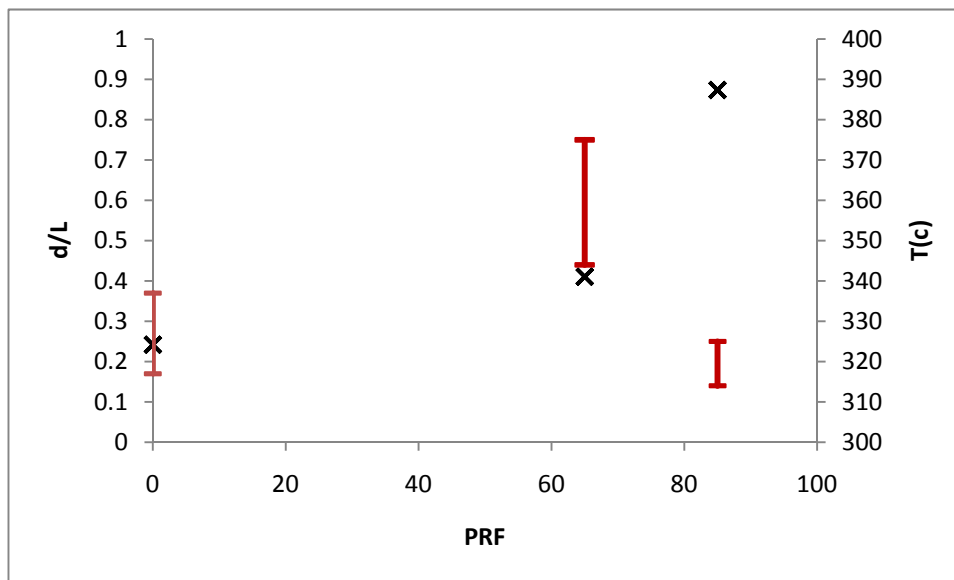


Figure 3-19: The Initial Cool Flame Positions and Temperature Rise of Trial #3

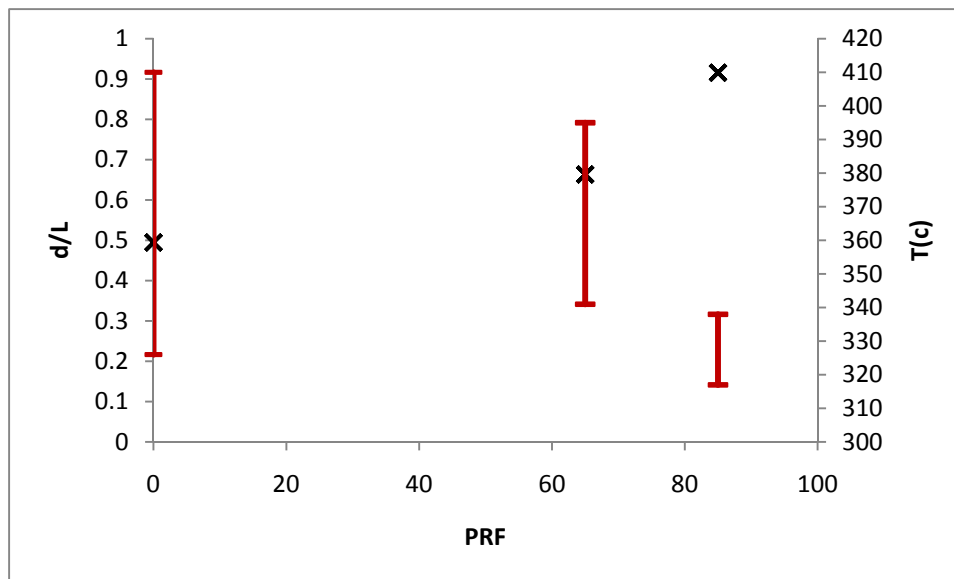


Figure 3-20: The Maximum Temperature Change Positions and Range of Trial #3

From Figures 3-16, 3-18 and 3-20, one finds that for all the trials, the maximum temperature rise positions were the same: PRF0 at 0.495, PRF65 at 0.663 and PRF85 at 0.916. The maximum temperature positions followed the similar pattern with the initial cool flame positions. The initial cool flame position and maximum temperature oscillation position of PRF65 were 0.168 behind those of PRF0. However, both of initial cool flame and maximum temperature oscillation position fell at 0.915, where almost the end of the reactor located. From Figure 3-22, one can see that the average temperature rise of PRF85 was the lowest among the three fuels. Therefore, it can be conjectured that there would have another maximum temperature oscillation position after 0.915 if the reactor was long enough, and that position would be 0.168 behind 0.915, which would be 1.084. That is, if one could make the reactor 26" long, one may see another maximum temperature oscillation at 25.75". In this case, due to the experimental setup constraint, the initial cool flame position would be a more reliable

From Figure 3-21, one can find that the initial temperature rising range did not follow an actual rule. In the first trial, the temperature rising range increased as the octane rating increased, but the second and third trial were different. PRF65 had the largest temperature rise in these two trials. However, it is obvious that in Figure 3-22, the maximum temperature rise in each run seemed favor lower octane rating. PRF0 had averagely 66C degree jump; PRF65 had 44C degree jump and PRF85 had 22C degree temperature jump. This phenomenon was due to the chemical structure of the fuel. Under same condition, lower PRF0 (n-heptane) has larger temperature jump than isooctane in a JSFR reactor (Ciajolo et al., 1998).

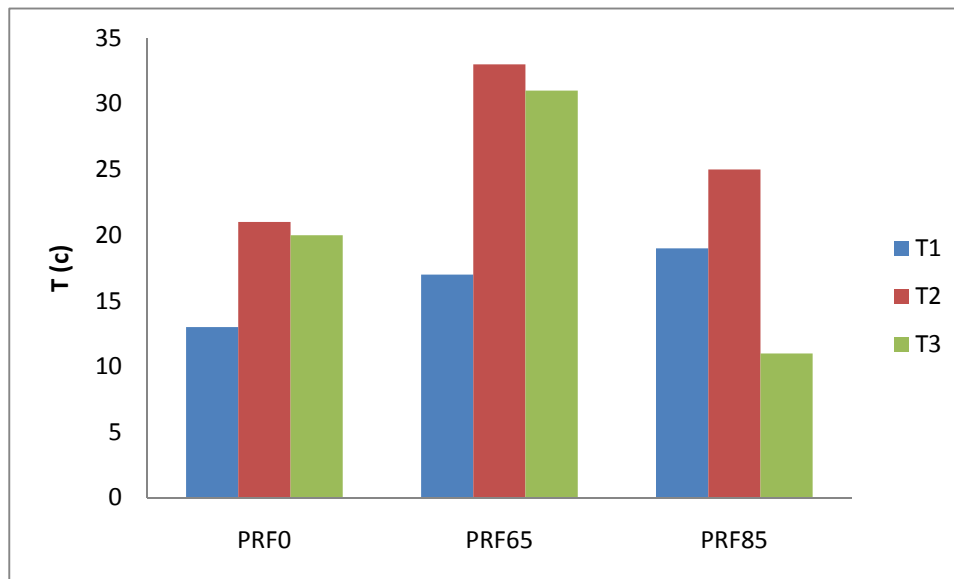


Figure 3-21: Initial Cool flame Temperature Rising Range for 3 Trials

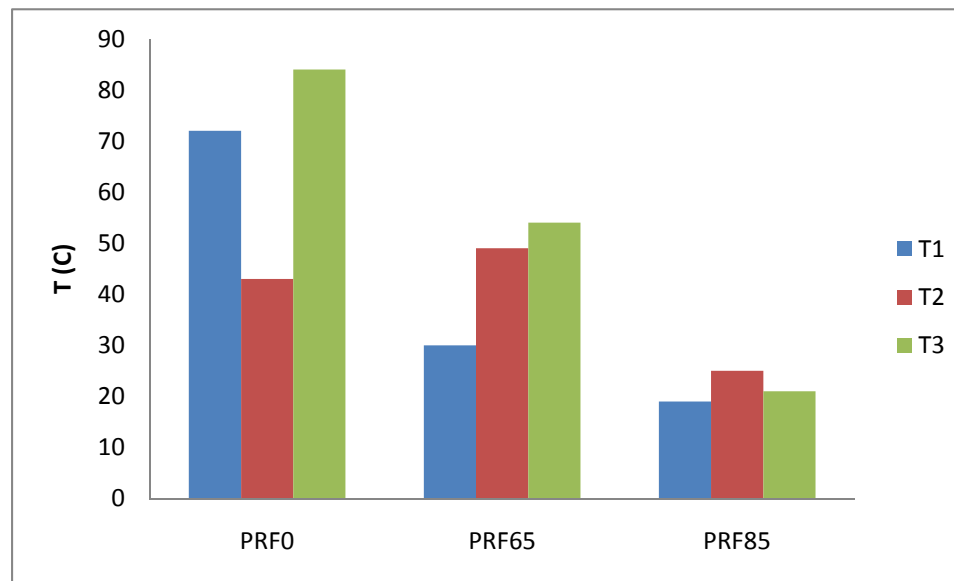


Figure 3-22: Maximum Temperature Rising Range for 3 Trials

## CHAPTER 4: CONCLUSIONS AND RECOMMENDATIONS

### **4.1. Summary of Conclusions**

Many methods were developed to determine octane number by correlating it with specific parameters. The present study built upon and modified from the experiments conducted by Stepankii et al. (1980). Major findings of this thesis research can be summarized as follows:

A first, surface property of reactor material was a key factor affecting the occurrence of cool flame. Borosilicate or pyrex is recommended. Second, visual light emission was not observed when the temperature oscillation was recorded or when the cool flame was present. Third, the temperature rise of the cool flame experiments was typically below 100C. Fourth, the experimental conditions that resulted in cool flame for PRF0, PRF65 and PRF85 were set to following conditions: air as oxidant, equivalence ratio equal to 1, inlet temperature at 182C, furnace temperature at 345C, and mixture velocity at 0.085m/s. Fifth, after performing the three trials under the above condition, one can tell that the lower the fuel octane number is, the larger temperature oscillation it would have. Lastly, the onset of cool flame seemed to be correlated with the fuel octane number and the position moved downstream when the fuel octane number was increased.

### **4.2 Future Works and Recommendations**

For the whole experiment, it took too much time to warm up (usually 2-3 hours). The heating system can be improved to speed up heating. Besides, a software having self-monitoring function is recommended. In this way, computer can find out the time of temperature oscillation and this will help to save time during the experiment as well as postprocessing. In the future, in addition to running more trials to obtain more data, one

can also use simulation softwares such as Fluent to simulate the experiment, and the results can be compared to actual experiment.

## REFERENCES

- Amann, C.A. "The Automotive Spark-Ignition Engine--An Historical Perspective." In *History of the Internal Combustion Engine* (E.F.C. Somerscales and A.A. Zagotta, editors). New York: American Society of Mechanical Engineers, 1989.
- Beasley, Donald E., and Richard S. Figliola. *Theory and Design for Mechanical Measurements*. 4 Har/Cdr ed. New York, NY: Wiley, 2005.
- Barusch, M.R. "Relation of Octane Number to Cool Flame Formation." *INDUSTRIAL AND ENGINEERING CHEMISTRY* 43.10 (1951): 2329.
- Drews, A. W. *Manual on Hydrocarbon Analysis (Astm Manual Series)*. Philadelphia: Astm International, 1998. Print.
- Elbe, Guenther von, and Bernard Lewis. *Combustion, Flames and Explosions of Gases, Third Edition*. 3 ed. Toronto: Academic Press, 1987.
- Gureev, A. A. "Determination of octane number based on parameters of reaction of cool-flame oxidation of hydrocarbons." *Chemistry and Technology of Fuels and Oils* 22.3 (1986): 147.
- Griffiths , J. F. , and S. M. Hasko. "Two-Stage Ignitions During Rapid Compression: Spontaneous Combustion in Lean Fuel-Air Mixtures." *Proceedings of the Royal Society A: Mathematical, Physical and sciences* 393.1805 (1984): 371-395.
- Gureev, A. A. , I. A. Dovlatov , and S. A. Kazaryan. "Monitoring knock resistance of fuels by an automatic instrument." *Chemistry and Technology of Fuels and Oils* 22.11 (1986): 610-612.
- Ingersoll, John G.. *Natural Gas Vehicles*. Boca Raton: Fairmont Pr, 1995.
- Jr, John J. Mcketta. *Encyclopedia of Chemical Processing and Design. Volume 1: Abrasives to Acrylonitrile*. Boca Raton: CRC, 1976.
- Kelly, Jeffrey J., Clyde H. Barlow, Thomas M. Jinguji, and James B. Callis. "Prediction of gasoline octane numbers from near-infrared spectral features in the range 660-1215 nm." *Analytical Chemistry* 61.4 (1989): 313-320.
- Mantashyan, A.A., P. S. Gukasyan, and R. H. Sayadyan. "Mechanism of cool-flame propane oxidation ." *Reaction Kinetics and Catalysis Letters* 11.3 (1979): 225-228.
- Nader, Ralph. "why they should tell you the octane rating of the gasoline you buy." *Popular Science* Apr. 1970: 54.



Pushkin, V. Yu., V. V. Kashmet, V. V. Blagoveshchenskii, V. I. Sakhnenko, V. A. Volkov, and S. V. Khotuntsova. "electrophysical methods of determination of the octane number of motor fuels." *Chemistry and Technology of Fuels and Oils* 38.4 (2002): 275-279.

Stepanskii, Ya. Yu. , N. P. Evmenenko, G. S. Yablonskii, and B. I. Kusovskii. "Correlation between octane number and certain parameters of gasoline oxidation." *Chemistry and Technology of Fuels and Oils* 10.1007/BF00727029. *Fuel and Oil Quality Evaluation Methods* (1980): 554-557.

Stepanskii, Ya. Yu. , G. S. Yablonskii , and V. I. Bykov. "Investigation of the characteristics of cold-flame oxidation of hydrocarbon mixtures as a function of their octane numbers ." *Combustion, Explosion, and Shock Waves* 18.1 (1982): 45-48.

Stepanskii, Ya. Yu. , N. P. Evmenenko , G. S. Yablonskii , and V. I. and V. I. Bykov1. "Self-oscillations in the cool-flame combustion of a model n-heptane-isooctane mixture ." *Reaction Kinetics and Catalysis Letters* 10.1007/BF02073501 (1980): 335-339.

TURNER, Stephen. R.. *An Introduction to Combustion: Concepts and Applications*. 2nd ed. New York: McGraw Hill Higher Education, 2000.